Applications in Engineering Science 2 (2020) 100009

Contents lists available at ScienceDirect

Applications in Engineering Science

journal homepage: www.elsevier.com/locate/apples

On the competition between interface energy and temperature in phase transition phenomena

Luca Bellino [a], Giuseppe Florio [a,b], Stefano Giordano [c], Giuseppe Puglisi [d,*]

[a] Politecnico di Bari, (DMMM) Dipartimento di Meccanica, Matematica e Management, Via Re David 200, Bari I-70125, Italy
[b] INFN, Sezione di Bari, I-70126, Italy
[c] Institute of Electronics, Microelectronics and Nanotechnology – UMR 8520, University of Lille, CNRS, Centrale Lille, ISEN, University of Valenciennes, LIA LICS/LEMAC, Lille F-59000, France
[d] Politecnico di Bari, (DICAR) Dipartimento di Scienza dell'Ingegneria Civile e dell'Architettura, Via Re David 200, Bari I-70125, Italy

ARTICLE INFO

Keywords:
Phase transition
Interfacial energy
Non local interactions
Size dependence
Temperature dependence

ABSTRACT

Phase nucleation and propagation phenomena can be characterized by a cooperative behavior regulated by non local interactions between the multistable domains and with the loading device. Cooperativity is often macroscopically witnessed by a stress-peak, distinguishing the nucleation from the propagation stress, and by a larger size of the first nucleated domain. When low dimensional scales are considered, both in nanostructures or single molecule behaviors, the interfacial energy can compete with entropic effects, leading to the experimental observation of a temperature dependent phase transition strategy. We propose a fully analytical model, in the framework of equilibrium Statistical Mechanics, measuring such energetic competition and temperature dependent behavior, that well reproduces important experimental evidences. The effectiveness of the model is successfully tested in predicting the temperature dependent phase transition behavior of shape memory nanowires.

1. Introduction

The description of finite microstructure domains evolution for multistable materials represents an important topic in material science that has been longly at the center of research activities for both its theoretical and technological importance (Allen and Cahn, 1979). Indeed, multi-states systems are of interest in several fields such as material science, biology, medicine, and engineering, both for natural and artificial materials. More recently, a large effort in this field has been devoted to the design of new high-performing metamaterials. In this case a successful new inverse approach is adopted, with a multistable microstructure designed to obtain the desired macroscopic behavior (Bilal et al., 2017; Shang et al., 2018).

In the thermomechanical three-dimensional case, the problem is quite complex and it asks for a description not only of the local structure of an interface, but also of its curvature and topological properties, necessary for the deduction of its excess energy (Angenent and Gurtin, 1989). The hypothesis of describing the microstructure evolution on the base of energy minimization was already proposed in the field of linear elasticity by Khachaturyan (1983) and coworkers. Later, Ericksen pioneering work (Ericksen, 1975) proposed a variational energetic approach in non linear elasticity theory with non convex energy densities. Grounded on this work, important theoretical advances in the field of modern continuum mechanics (Ball and James, 1989) and calculus of variation (Müller, 1999) successfully described basic aspects of phase transitions and of associated effects at the microstructure level. In particular, the analysis of the complex problem of minimization of the non (quasi) convex energy allowed important results regarding the phase fraction, the orientation of the interfaces and the stress corresponding to the phase evolution. Nonetheless, continuum variational approaches minimizing the elastic energy density are not able to capture important aspects unless they introduce interfacial energy effects and non-local interactions. As a matter of fact, these energetic contributions are crucial for a detailed description of the observed microstructure evolution (Shaw and Kyriakides, 1997) and they are fundamental not only from a theoretical point of view, but also for a correct portrayal of the material behavior and for the design of new materials (Ren and Truskinovsky, 2000). In particular, the minimization of the (non-convex, bulk) elastic energy only cannot describe the existence of internal length scales regulating the effective observed phenomena leading to discrete processes of transition with nucleation and propagation of finite domains (see Refs. Abeyaratne et al. (1996); Benichou and Givli (2013) and references therein). Based on these observations, different 'augmented' energetic models have been proposed. Schematically, on one side higher

* Corresponding author.
E-mail addresses: luca.bellino@poliba.it (L. Bellino), giuseppe.florio@poliba.it (G. Florio), stefano.giordano@univ-lille.fr (S. Giordano), giuseppe.puglisi@poliba.it (G. Puglisi).

https://doi.org/10.1016/j.apples.2020.100009
Received 11 July 2020; Accepted 20 July 2020
Available online xxx

gradient (Carr et al., 1984; Triantafyllidis and Bardenhagen, 1993) (antiferromagnetic) energy terms, representing surface energy contributions, have been added to the energy density, possibly deduced as a result of compatibility effects as in the case of polymer necking in the classical work presented in Ref. (Coleman, 1983). On the other side, non local (ferromagnetic and antiferromagnetic) energy terms have been considered, thus introducing the desired length scale needed to describe the insurgence of periodic microstructures tipically observed in solid-solid martensitic phase transitions (see Refs. Müller, 1999; Ren and Truskinovsky, 2000 and references therein).

Starting from the pioneering work in Ref. Müller and Villaggio (1977), a parallel framework in the field of discrete mechanics was proposed. In the simpler setting, one can consider a lattice of elements with non convex energy densities and the presence of an intrinsic discreteness length-scale (Fedelich and Zanzotto, 1992). As a result, it is possible to describe fundamental properties such as energy barriers, metastable states, quasi-plastic and pseudo-elastic behaviors (Puglisi and Truskinovsky, 2000; 2005). On the other hand, also this approach was not able to distinguish between different microstructures with the same phase fraction and, therefore, important details of the nucleation and phase fronts evolution phenomena could not be described. The model has been generalized by considering non local energy terms in Refs. Puglisi (2006, 2007); Truskinovsky and Vainchtein (2004) where the authors were able to describe the important effect of a stress peak in order to distinguish the different phenomena of nucleation and propagation. In analogy with higher gradient approaches in elasticity, only single wall solutions with a fully cooperative phase transition could be described. On the other hand, in Refs. Puglisi (2006, 2007) a more detailed analysis of the influence of boundary conditions let the author energetically distinguish between internal and boundary nucleation, with possible two phase fronts. These features are often observed for example in polymer necking localization phenomena. Moreover, the model has been extended to the case of configurational transitions in protein macromolecules to study the successive unfolding events observed in protein stretched under single molecule force spectroscopy experiments (De Tommasi et al., 2013; Manca et al., 2013). In this case the two energy wells correspond to two different configurations of the protein domains, with a folded → unfolded transition. Finally, based on multiscale approaches this class of models has been adopted to deduce the macroscopic features of protein materials in Refs. De Tommasi et al. (2015); Puglisi et al. (2017), showing a significant predictivity of the experimental behavior.

In this paper we are interested in a description of the possibility of entropic effects delivering a temperature dependence of the stress peak, of the size of nucleation domain and, in general, of the cooperative nature of the transition. Schematically, temperature effects can have crucial effects in the behavior of multistble materials for three different reasons. First, increasing or decreasing temperature may result in a change of the potential energy of the different possible configurations such as in the case of Shape Memory Alloys (SMA) (Tanaka et al., 1986). Second, temperature effects regulate the capability of overcoming energy barriers, thus influencing the key role of metastability, hysteresis and rate effects (see *e.g.* Refs. Keller and Cheng (1998); Puglisi and Truskinovsky (2002); Tanaka et al. (1986)). Third, when rate effects are excluded and the system is able to relax to the global minimum of the free energy, the entropic term can favor solutions with multiple interfaces (Müller and Seelecke, 2001). This is particularly relevant when the transition is controlled by low enthalpies such as in the case of conformational transitions of units with weak bonds in biological materials or when the scale of the system is very small. In this case, we have a competition between the interfacial energy (favoring solutions with low numbers of interfaces) and entropic energy terms (favoring solutions with a high number of interfaces). As a matter of fact, under these hypotheses, the behavior of the system is described by the expectation values of relevant observables with respect to the thermal fluctuations and, therefore, the correct framework for the analysis is given by a Statistical Mechanics approach.

Specifically, by extending the results in Refs. Puglisi (2006, 2007) and including temperature effects, in this paper we consider a prototypical example constituted by a chain of elements with bistable potentials, describing a material with two distinct phases (i.e folded → unfolded configurations in a macromolecule or austenitic and martensitic phases in SMA). In analogy with the continuous model with higher order gradient energy terms (Triantafyllidis and Bardenhagen, 1993), here we mimic the important role of interfacial energy by considering next to nearest neighbor (NNN) interactions (see Fig. 1). The zero temperature (mechanical limit) behavior of this system was studied in Refs. Puglisi (2006, 2007); Truskinovsky and Vainchtein (2004). The effectiveness of Statistical Mechanics approach in describing thermal effects observed in multistable systems has been recently shown in a series of papers (Bellino et al., 2019; Benedito and Giordano, 2018a; 2018b; 2020; Efendiev and Truskinovsky, 2010; Florio and Puglisi, 2019; Giordano, 2017; 2018; Makarov, 2009). In these papers several theoretical and applied problems regarding entropic effects and boundary conditions have been analyzed. In particular, the authors have focussed on the analysis of the behavior of protein macromolecules represented as a system of bistable domains undergoing conformational folded → unfolded transition. In the same spirit, in the recent paper (Florio et al. 2020), these models have been used to consider the important temperature effects to study a peeling behavior such as in geckoes pad, thus extending the approach in Ref. Puglisi and Truskinovsky (2013). In this case, the bistable elements are breakable so that the second state (detached state) is characterized by zero force and stiffness. Such type of models have been widely adopted also in the literature of DNA denaturation in analogy with the Peyrard-Bishop model (Peyrard, 2004).

The paper is organized as it follows. In Section 2 we introduce the model. In Section 3 we study the purely mechanical (zero temperature) case and obtain the stress strain relation at equilibrium. In Sections 4 and 5 we consider the effects of temperature in the cases of applied stress (Gibbs ensemble, soft device) and strain (Helmholtz ensemble, hard device), respectively. In Section 6 we compare the predictions of our model with results obtained using Molecular Dynamics (MD) simulations on shape memory nanowires. In Section 7 we discuss the results and draw the conclusions with possible perspectives.

2. Model

Following the approaches of Refs. Puglisi (2006, 2007); Truskinovsky and Vainchtein (2004), let us consider a chain of $n+1$ points, schematized in Fig. 1, linked by nearest-neighborhood (NN) bistable units with reference length l and next-to-nearest-neighbor harmonic springs with natural length $2l$. Each NN link is characterized by a two wells energy, corresponding to two different material states. They can represent two different phases (Puglisi and Truskinovsky, 2000), as in solid-solid phase transition, or two different conformational (folded and unfolded) states as in the case of unfolding phenomena in protein molecules (De Tommasi et al., 2013). Besides, in the limit case when the second well degenerates to a constant energy we can describe the behavior of breakable bonds as in Ref. Puglisi and Truskinovsky (2013).

After introducing the "spin" variable S_j, that defines the phase of each unit as

$$S_j = \begin{cases} -1 & \text{phase one} \\ +1 & \text{phase two} \end{cases}, \tag{1}$$

we may write the potential energy of the NN springs (see Fig. 1(c)) as it follows:

$$\phi_{NN}(S_j, \varepsilon_j) = \frac{1}{2} k\, l \left[\left(\varepsilon_j + \varepsilon_0\right)^2 \frac{\left(1 - S_j\right)}{2} + \left(\zeta \left(\varepsilon_j - \varepsilon_0\right)^2 + 2\eta \right) \frac{\left(1 + S_j\right)}{2} \right], \quad j = 1, \ldots, n, \tag{2}$$

where $-\varepsilon_0$ and ε_0 are the reference strains of the first and second well, respectively, k/l is the stiffness of the first well (k has the dimension

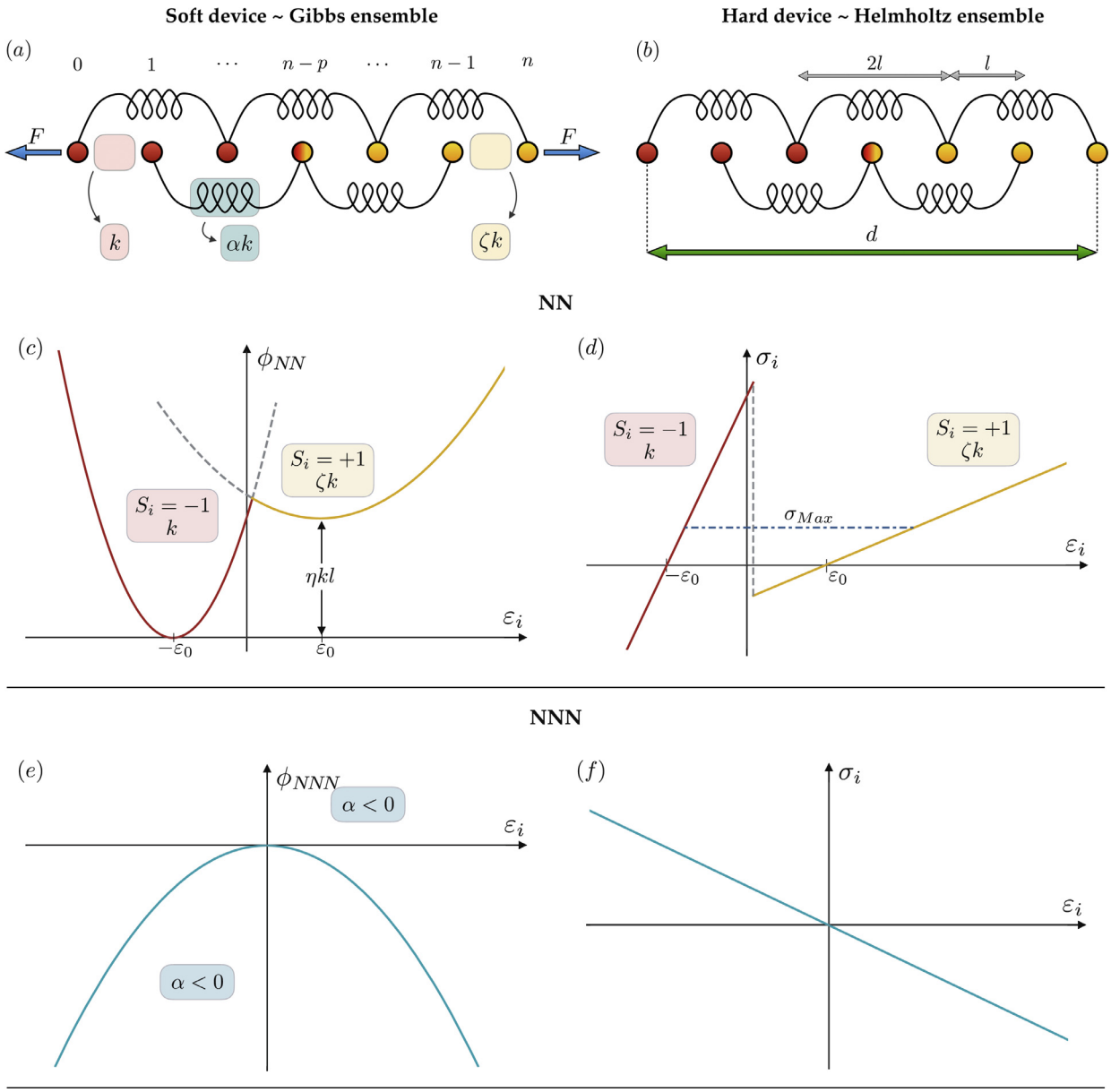

Fig. 1. Scheme of the mechanical model in the two considered cases of (a) assigned force F and (b) assigned total displacement d. Energies for the NN (c) and NNN (e) units and corresponding force–displacement diagrams are in (d) and (f), respectively.

of a force), $\zeta k/l$ is the stiffness of the second phase and η measures the transition energy with respect to the ground state.

Next, we consider the simplest case of non local interactions by introducing NNN harmonic oscillators of length $2l$, with energy

$$\phi_{NNN}(\varepsilon_j,\varepsilon_{j+1}) = \frac{1}{2}\alpha\, k\, l\, (\varepsilon_j+\varepsilon_{j+1})^2, \quad j=1,\dots,n-1, \tag{3}$$

where α measures the relative stiffness of the non local vs local springs. Observe that while in this paper we are interested in the (concave) case with $\alpha<0$, when non local energy terms penalize interfaces formation (ferromagnetic hypothesis), the following calculations hold true also in the (convex) case with $\alpha>0$, when the interfaces formation is favored (antiferromagnetic hypothesis). Moreover, while we deduce our theoretical relations for general values of α, with the aim of getting analytic results we then focus on the case $|\alpha|\ll 1$, so that the NNN energy represents a perturbative term that let us distinguish between solutions with the same phase fraction, but with different number of interfaces.

The total (adimensionalized with respect to lk) energy of the system is then

$$\begin{aligned}\varphi(\{S_j\},\{\varepsilon_j\}) &= \frac{1}{2}\left\{\sum_{j=1}^{n}\left[(\varepsilon_j+\varepsilon_0)^2\frac{(1-S_j)}{2}+\left(\zeta(\varepsilon_j-\varepsilon_0)^2+2\eta\right)\frac{(1+S_j)}{2}\right]\right.\\ &\left.+\sum_{j=1}^{n-1}\alpha\left(\varepsilon_j+\varepsilon_{j+1}\right)^2\right\}.\end{aligned} \tag{4}$$

With the aim of simplifying the notation, we may introduce the following functions of the spin variable:

$$L(S_j)=\begin{cases}1 & \text{if} \quad S_j=-1\\ \zeta & \text{if} \quad S_j=+1\end{cases},\quad m(S_j)=\begin{cases}-\varepsilon_0 & \text{if} \quad S_j=-1\\ \zeta\varepsilon_0 & \text{if} \quad S_j=+1\end{cases},$$
$$q(S_j)=\begin{cases}\varepsilon_0^2/2 & \text{if} \quad S_j=-1\\ \zeta\varepsilon_0^2/2+\eta & \text{if} \quad S_j=+1\end{cases}. \tag{5}$$

Accordingly, we may define the vectors

$$\boldsymbol{\varepsilon}=\begin{pmatrix}\varepsilon_1\\ \cdots\\ \varepsilon_j\\ \cdots\\ \varepsilon_n\end{pmatrix},\qquad \boldsymbol{s}=\begin{pmatrix}S_1\\ \cdots\\ S_j\\ \cdots\\ S_n\end{pmatrix},\qquad \boldsymbol{m}=\begin{pmatrix}m_1\\ \cdots\\ m_j\\ \cdots\\ m_n\end{pmatrix},\qquad \boldsymbol{q}=\begin{pmatrix}q_1\\ \cdots\\ q_j\\ \cdots\\ q_n\end{pmatrix},\qquad \boldsymbol{1}=\begin{pmatrix}1\\ \cdots\\ \cdots\\ \cdots\\ 1\end{pmatrix}, \tag{6}$$

where $m_j = m(S_j)$, $q_j = q(S_j)$ and each element of the vector $\boldsymbol{s}$ is the "spin" of the jth NN unit. In addition, we may introduce the matrices

$$\boldsymbol{L}=\begin{pmatrix}L_1 & & & & \boldsymbol{0}\\ & \ddots & & & \\ & & L_j & & \\ & & & \ddots & \\ \boldsymbol{0} & & & & L_n\end{pmatrix},\qquad \boldsymbol{A}=\begin{pmatrix}1 & 1 & & & \boldsymbol{0}\\ 1 & 2 & 1 & & \\ & \ddots & \ddots & \ddots & \\ & & 1 & 2 & 1\\ \boldsymbol{0} & & & 1 & 1\end{pmatrix}, \tag{7}$$

where $L_j = L(S_j)$. Finally, by using (5), (6) and (7) we can compactly rewrite the energy of the system as

$$\varphi(\boldsymbol{s},\boldsymbol{\varepsilon})=\frac{1}{2}\boldsymbol{J}\boldsymbol{\varepsilon}\cdot\boldsymbol{\varepsilon}-\boldsymbol{m}\cdot\boldsymbol{\varepsilon}+q, \tag{8}$$

where $\boldsymbol{J}=\boldsymbol{J}(\boldsymbol{s})=\boldsymbol{L}(\boldsymbol{s})+\alpha\boldsymbol{A}$, $\boldsymbol{m}=\boldsymbol{m}(\boldsymbol{s})$ and $q=q(\boldsymbol{s})=\boldsymbol{q}(\boldsymbol{s})\cdot\boldsymbol{1}$.

Remark. While previous description shows that the following analysis can be extended to the full general case, in order to focus on the physical results and get simply interpretable analytical formulas, in the following we study the case of $\zeta = 1$ and $\eta = 0$, *i.e.* we assume identical wells with no energy gap. Thus, with the aforementioned hypothesis we have

$$\boldsymbol{L}=\boldsymbol{I},\qquad q=n\,\varepsilon_0^2/2,\qquad \boldsymbol{m}=\varepsilon_0\boldsymbol{s}. \tag{9}$$

Observe that in the following we first obtain all the formulas without this assumption in terms of $\boldsymbol{J}$ and $\boldsymbol{m}$ and then we specialize them to the simpler case of (9).

3. Equilibrium

With the aim of getting physical insight into the problem of non local interactions and study their role in the proposed model, in this section we summarize the equilibrium configurations of the system when temperature effects are neglected. Here we study both the case of soft and hard devices, that, as demonstrated in Ref. Bellino et al. (2019), can be considered as limit regimes of a general problem in which the stiffness of the pulling device regulates the effective boundary conditions. We refer to Refs. Puglisi (2006, 2007) for a more detailed analysis when also the interaction with the loading experimental apparatus is considered.

3.1. Soft device

First, let us consider the case of soft device with applied force F (Fig. 1(a)). The potential energy of the systems is

$$g(\boldsymbol{s},\boldsymbol{\varepsilon},\sigma)=\varphi(\boldsymbol{s},\boldsymbol{\varepsilon})-\sigma\sum_{j=1}^{n}\varepsilon_j=\frac{1}{2}\boldsymbol{J}\boldsymbol{\varepsilon}\cdot\boldsymbol{\varepsilon}-(\boldsymbol{m}+\sigma\boldsymbol{1})\cdot\boldsymbol{\varepsilon}+q, \tag{10}$$

where $\sigma = F/k$ is the adimensional load.

Equilibrium at assigned phase configuration $\boldsymbol{s}$ gives

$$\frac{\partial g(\boldsymbol{s},\boldsymbol{\varepsilon},\sigma)}{\partial\boldsymbol{\varepsilon}}=\boldsymbol{J}\boldsymbol{\varepsilon}-(\boldsymbol{m}+\sigma\boldsymbol{1})=\boldsymbol{0}. \tag{11}$$

Therefore, the equilibrium strains are

$$\boldsymbol{\varepsilon}_{eq}=\boldsymbol{J}^{-1}(\boldsymbol{m}+\sigma\boldsymbol{1}), \tag{12}$$

corresponding to an average strain $\bar{\varepsilon} := \frac{1}{n}\sum_{j=1}^{n}\varepsilon_j$ and energy

$$\begin{aligned}\bar{\varepsilon}_{eq}&=\frac{1}{n}\left(\boldsymbol{\varepsilon}_{eq}\cdot\boldsymbol{1}\right)=\frac{1}{n}\left[\boldsymbol{J}^{-1}(\boldsymbol{m}+\sigma\boldsymbol{1})\cdot\boldsymbol{1}\right],\\ g_{eq}&=-\frac{1}{2}\boldsymbol{J}^{-1}(\boldsymbol{m}+\sigma\boldsymbol{1})\cdot(\boldsymbol{m}+\sigma\boldsymbol{1})+q.\end{aligned} \tag{13}$$

Following Ref. Puglisi (2006), the inverse of the tridiagonal Hessian matrix $\boldsymbol{J}$ (non-singular in the hypothesis of small α) can be expressed as

$$\boldsymbol{J}^{-1}=\sum_{j=0}^{\infty}(-\alpha)^j\boldsymbol{L}^{-1}(\boldsymbol{A}\boldsymbol{L}^{-1})^j. \tag{14}$$

For small α, taking into account that by using (9) we have $\boldsymbol{L}=\boldsymbol{I}$, (14) gives

$$\boldsymbol{J}^{-1}\simeq\boldsymbol{I}-\alpha\boldsymbol{A}. \tag{15}$$

Then, let us introduce the identities

$$\begin{aligned}&\boldsymbol{s}\cdot\boldsymbol{s}=n, && \boldsymbol{A}\boldsymbol{s}\cdot\boldsymbol{s}=4(n-i-1),\\ &\boldsymbol{s}\cdot\boldsymbol{1}=2\,p-n, && \boldsymbol{A}\boldsymbol{s}\cdot\boldsymbol{1}=4(2\,p-n)-2(S_1+S_n),\\ &\boldsymbol{1}\cdot\boldsymbol{1}=n, && \boldsymbol{A}\boldsymbol{1}\cdot\boldsymbol{1}=4(n-1),\end{aligned} \tag{16}$$

where p the *is number of elements in the second phase* and i is *the number of interfaces*, *i.e.* the number of times NN adjacent links have different phases, S_1 and S_n assign the phase of the boundary elements. Finally, by using (9), (15) and (16), Eq. (13) can be rewritten as

$$\begin{aligned}\bar{\varepsilon}_{eq}&=(1-4\alpha)\left[\sigma+\left(2\chi-1\right)\varepsilon_0\right]+\frac{2\alpha}{n}\left[2\sigma+\left(S_1+S_n\right)\varepsilon_0\right],\\ \frac{g_{eq}}{n}&=-(1-4\alpha)\left[\frac{\sigma^2}{2}+\left(2\chi-1\right)\varepsilon_0\sigma\right]\\ &\quad-\frac{2\alpha}{n}\left[\sigma^2+\left(S_1+S_n\right)\varepsilon_0\sigma+i\,\varepsilon_0^2+\left(n-1\right)\varepsilon_0^2\right],\end{aligned} \tag{17}$$

where $\chi := p/n$ is the *phase fraction*.

Observe that the equilibrium configurations in (17), when NNN interactions are not considered ($\alpha = 0$), only depend on the phase fraction χ. On the contrary, when non local terms are introduced, the number of interfaces distinguishes configurations with the same phase fraction. In particular, solutions with a larger number of interfaces are energetically penalized. It is easy to verify that the *global minimum* of the energy is attained when all bistable units are in the first phase for $\sigma < 0$ and in the second phase when $\sigma > 0$, as shown in Fig. 2(a). Consequently, under the so called Maxwell hypothesis, when the configurations of the system correspond always to the global energy minimum, we observe that as the force is increased the chain undergoes an "instantaneous" transition from the homogeneous state in the first phase to the homogeneous state in the second one with a fully cooperative phase transition and no interfaces.

3.2. Hard device

Consider now the case of assigned total displacement d, as schematized in Fig. 1(b), and introduce its dimensionless measure

$$\delta=\frac{d}{l}=\sum_{j=1}^{n}\varepsilon_j=\boldsymbol{\varepsilon}\cdot\boldsymbol{1}. \tag{18}$$

The equilibrium strain equations at fixed configuration $\boldsymbol{s}$ are again given by (12), where σ is the Lagrange multiplier measuring the force conjugate to the fixed total displacement in (18). By using Eq. (9), in the case of small α (see Eqs. (15)), (18) can be rewritten as

$$\begin{aligned}\bar{\varepsilon}&=\frac{\delta}{n}=\frac{1}{n}\left[\boldsymbol{J}^{-1}\left(\boldsymbol{m}+\sigma_{eq}\boldsymbol{1}\right)\cdot\boldsymbol{1}\right]\\ &\simeq\frac{1}{n}\left[(\boldsymbol{1}\cdot\boldsymbol{1}-\alpha\boldsymbol{A}\boldsymbol{1}\cdot\boldsymbol{1})\sigma_{eq}+(\boldsymbol{s}\cdot\boldsymbol{1}-\alpha\,\boldsymbol{A}\boldsymbol{s}\cdot\boldsymbol{1})\varepsilon_0\right],\end{aligned} \tag{19}$$

where we indicate by σ_{eq} the equilibrium stress. Accordingly, we obtain the equilibrium energy

$$\begin{aligned}\varphi_{eq}&=-\frac{1}{2}\boldsymbol{J}^{-1}\left(\boldsymbol{m}+\sigma_{eq}\boldsymbol{1}\right)\cdot\left(\boldsymbol{m}+\sigma_{eq}\boldsymbol{1}\right)+q+\delta\,\sigma_{eq}\\ &\simeq-\frac{1}{2}\left(\boldsymbol{1}\cdot\boldsymbol{1}-\alpha\boldsymbol{A}\boldsymbol{1}\cdot\boldsymbol{1}\right)\sigma_{eq}^2\\ &\quad-\left(\boldsymbol{s}\cdot\boldsymbol{1}-\alpha\,\boldsymbol{A}\boldsymbol{s}\cdot\boldsymbol{1}-\delta\right)\varepsilon_0\,\sigma_{eq}+\frac{1}{2}\alpha\,\varepsilon_0^2\,\boldsymbol{A}\boldsymbol{s}\cdot\boldsymbol{s}.\end{aligned} \tag{20}$$

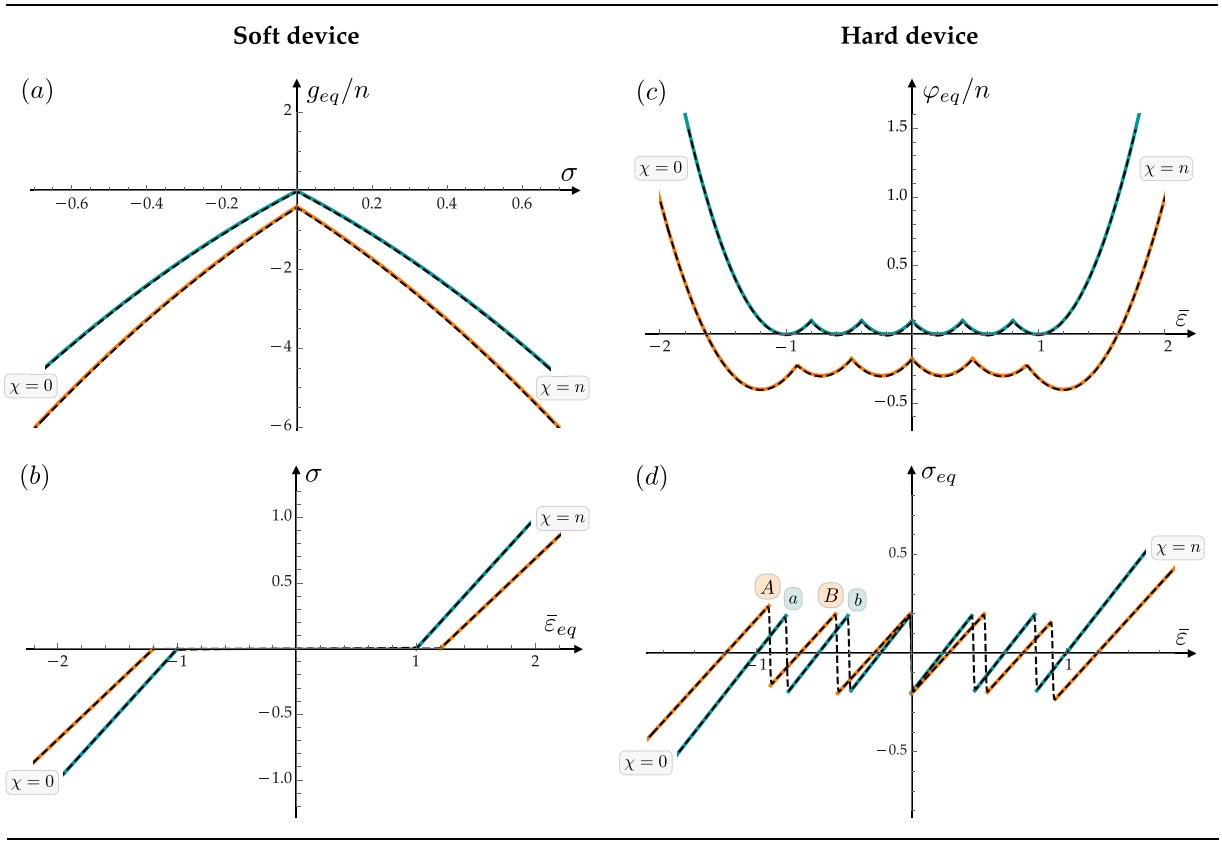

Fig. 2. Mechanical equilibrium. Energies and stress-strain diagrams in the soft (a),(b) and hard (c),(d) device. Cyan curves represent the cases when only NN interactions are considered, orange curves show the behavior with the presence of non local terms. Dashed black lines are calculated with the Statistical Mechanics approach when the temperature goes to zero (see Section 4,5). Parameter: $n = 5$, $\alpha = 0$ in cyan curves and $\alpha = -0.05$ in the orange ones, $\tilde{\beta} \to \infty$ in the black dashed lines, $\varepsilon_0 = 1$.

Eventually, by using (16) we obtain

$$\sigma_{eq} = \frac{\bar{\varepsilon} - \left[(1-4\alpha)(2\chi - 1) + \frac{2\alpha}{n}(S_1 + S_n)\right]\varepsilon_0}{1 - \frac{4\alpha}{n}(n-1)}, \tag{21}$$

and the equilibrium energy per element is given by

$$\frac{\varphi_{eq}}{n} = \frac{1}{2}\left\{ \frac{\left[((1-4\alpha)(2p/n - 1) + \frac{2\alpha}{n}(S_1 + S_n))\varepsilon_0 - \bar{\varepsilon}\right]^2}{1 - \frac{4\alpha}{n}(n-1)} + \frac{4\alpha}{n}(n - i - 1)\varepsilon_0^2 \right\}. \tag{22}$$

In this case the *global minima* of the energy with respect to the assigned rescaled displacement δ are given by solutions either homogeneous or with one single interface, as shown in Fig. 2(c). More in details, in agreement with well known experimental observations, under the hypothesis of hard device the system changes state between the two homogeneous phase branches following a 'sawtooth' equilibrium path. Interestingly, the stress corresponding to the nucleation of the new phase (point A in Fig. 2(d)) is higher than the stress corresponding to the propagation of the interface (*e.g.* point B in figure). It is important to notice that this effect is not observed in absence of non local interactions (points a and b). Moreover, one may show that by increasing the value of n or of the non local energy α the nucleation can correspond to the cooperative transition of more elements. Such behavior is discussed in detail in Ref. Puglisi (2007), whereas here we are interested in the energetic competition of surface energy terms (measured by the parameter α) and entropic energy terms, so that we postpone the discussion to the following sections.

4. Applied stress: Gibbs ensemble

To describe the important effect of temperature, consider now our prototypical model with non local interactions in the framework of equilibrium Statistical Mechanics. Under isotensional conditions (*i.e* assigned stress σ, soft device), we derive the canonical partition function in the Gibbs ensemble (denoted by the subscript $\mathscr{G}$), in order to study the system in thermal equilibrium (Weiner, 1983). By definition and by using the energy in (10), we have

$$\mathcal{Z}_{\mathscr{G}}(\sigma) = \sum_{\{S_j\}} \int_{\mathbb{R}^n} e^{-\tilde{\beta} g} \mathrm{d}\boldsymbol{\varepsilon} = \sum_{\{S_j\}} \int_{\mathbb{R}^n} e^{-\tilde{\beta}\left(\frac{1}{2}\boldsymbol{J}\boldsymbol{\varepsilon}\cdot\boldsymbol{\varepsilon} - (\boldsymbol{m}+\sigma\mathbf{1})\cdot\boldsymbol{\varepsilon} + q\right)} \mathrm{d}\boldsymbol{\varepsilon}, \tag{23}$$

where $\tilde{\beta} = \beta l k$ and $\beta = 1/(k_B T)$, with k_B the Boltzmann constant and T the absolute temperature. Here, we have summed over the discrete spin variables and we integrated the continuous strains.

Remark. It is important to point out that by following Refs. Efendiev and Truskinovsky (2010), Florio et al. (2020), in order to obtain analytical results we assume that the two wells are extended beyond the spinodal point so that at the given configuration $\boldsymbol{s}$ we may integrate all the strain all over $\mathbb{R}$ and avoid error functions. In Florio and Puglisi (2019) the authors numerically showed that in the temperature regimes of interest for real experiments this approximation does not influence the energy minimization.

A straightforward evaluation of the Gaussian integral leads to

$$\mathcal{Z}_{\mathscr{G}}(\sigma) = \sum_{\{S_j\}} \sqrt{\frac{(2\pi)^n}{\det(\boldsymbol{J})}} e^{-\tilde{\beta}\left(-\frac{1}{2}\boldsymbol{J}^{-1}(\boldsymbol{m}+\sigma\mathbf{1})\cdot(\boldsymbol{m}+\sigma\mathbf{1}) + q\right)}, \tag{24}$$

where, as expected, at the exponent we find the equilibrium energy in (13). Accordingly, preserving the same first order approximation

in (15) with α kept small and by using (9), we obtain

$$\mathcal{Z}_{\mathscr{G}}(\sigma) \simeq \sqrt{\frac{(2\pi)^n}{\det(\boldsymbol{I}-\alpha\boldsymbol{A})}} \sum_{\{S_j\}} e^{\beta\left\{\frac{1}{2}[(\varepsilon_0 s+\sigma\mathbf{1})\cdot(\varepsilon_0 s+\sigma\mathbf{1})-\alpha\boldsymbol{A}(\varepsilon_0 s+\sigma\mathbf{1})\cdot(\varepsilon_0 s+\sigma\mathbf{1})]-q\right\}}. \tag{25}$$

Remark. While (25) gives numerically the possibility of evaluating the partition function, we may observe that by using (16), in the approximation of small α the exponent in (25) reduces to the equilibrium energy in (17). This expression depends on the configuration S_j only by the number of unfolded elements p, the number of interfaces i and by the boundary phases S_1 and S_n. In order to obtain explicit formulas of the partition function and optimize the numerical calculation, we can neglect the contribution of the boundary energy terms in (17) given by $-\frac{2\alpha}{n}(S_1+S_n)$, while keeping the contribution of S_1 and S_n in the evaluation of the phase fraction $\chi = p/n$ and of the number of interfaces i. This is justified by the observation that this energy term is proportional to α/n and can be shown to be small for large n and small enough α as compared with the other energy terms. We refer to Refs. Puglisi (2006, 2007) for a more detailed discussion about boundary effects, that instead can be particularly important when temperature effects are neglected.

Under the described assumption we need to evaluate the combinatorial coefficient $\mathcal{W}_{p,i}$ counting the number of configurations corresponding to the values of p and i. Following the approach in Refs. Denisov and Hänggi (2005); Ising (1925); Seth (2016), it is possible to obtain that

$$\mathcal{W}_{p,i} = \begin{cases} \mathcal{W}_{odd}(p,i) & \text{if } i \text{ odd}, \\ \mathcal{W}_{even}(p,i) & \text{if } i \text{ even}, \\ 1 & \text{if } i=0, p=0 \text{ or } p=n, \\ 0 & \text{if } i=0, 0<p<n, \end{cases} \tag{26}$$

with

$$\mathcal{W}_{odd}(p,i) = 2\binom{p-1}{\frac{i-1}{2}}\binom{n-p-1}{\frac{i-1}{2}}\Theta\left(p-\frac{i+1}{2}\right)\Theta\left(n-p-\frac{i+1}{2}\right), \tag{27}$$

and

$$\mathcal{W}_{even}(p,i) = \binom{p-1}{\frac{i}{2}}\binom{n-p-1}{\frac{i}{2}-1}\Theta\left(p-\frac{i+2}{2}\right)\Theta\left(n-p-\frac{i}{2}\right) + \binom{n-p-1}{\frac{i}{2}}\binom{p-1}{\frac{i}{2}-1}\Theta\left(p-\frac{i}{2}\right)\Theta\left(n-p-\frac{i+2}{2}\right), \tag{28}$$

where Θ is the Heaviside step function ($\Theta(x)=0$ if $x<0$ and $\Theta(x)=1$ if $x\geq 0$).

Finally, using the combinatorial coefficient in (26), we obtain the canonical partition function in the Gibbs ensemble

$$\mathcal{Z}_{\mathscr{G}}(\sigma) = \mathcal{K}_{\mathscr{G}} \sum_{p=0}^{n}\sum_{i=0}^{n-1} \mathcal{W}_{p,i}\, e^{\Gamma_{p,i}(\sigma)}, \tag{29}$$

where

$$\mathcal{K}_{\mathscr{G}} = \sqrt{\frac{(2\pi)^n}{\det(\boldsymbol{I}-\alpha\boldsymbol{A})}} \tag{30}$$

is a noninfluential constant and the exponent, by using (16), can be written as

$$\Gamma_{p,i}(\sigma) = \frac{n\tilde{\beta}}{2}\left\{(1-4\alpha)\left[4\,\frac{p}{n}\,\varepsilon_0\,\sigma + \left(\sigma-\varepsilon_0\right)^2\right] + \frac{4\alpha}{n}\,i\,\varepsilon_0^2 - \varepsilon_0^2 + \frac{4\alpha}{n}(\varepsilon_0^2+\sigma^2)\right\}. \tag{31}$$

By definition, the Gibbs free energy is (Manca et al., 2012; Weiner, 1983)

$$\mathcal{G}(\sigma) = -\frac{1}{\tilde{\beta}}\ln \mathcal{Z}_{\mathscr{G}}(\sigma), \tag{32}$$

and one may now evaluate the expectation value of the strain, which is the conjugate variable (up to n since $\delta = n\bar{\varepsilon}$) to the applied force σ, as

$$\langle\bar{\varepsilon}\rangle = -\frac{1}{n}\frac{\partial}{\partial\sigma}\mathcal{G}(\sigma) = \frac{1}{n\tilde{\beta}\mathcal{Z}_{\mathscr{G}}(\sigma)}\frac{\partial}{\partial\sigma}\mathcal{Z}_{\mathscr{G}}(\sigma), \tag{33}$$

that takes the form

$$\langle\bar{\varepsilon}\rangle = (1-4\alpha)\left[2\varepsilon_0\langle\chi\rangle_{\mathscr{G}} + [\sigma-\varepsilon_0]\right] + \frac{4\alpha}{n}\sigma, \tag{34}$$

$$\langle\chi\rangle_{\mathscr{G}} = \frac{\sum_{p=0}^{n}\sum_{i=0}^{n-1}\mathcal{W}_{p,i}\,\chi\, e^{\Gamma_{p,i}(\sigma)}}{\sum_{p=0}^{n}\sum_{i=0}^{n-1}\mathcal{W}_{p,i}\, e^{\Gamma_{p,i}(\sigma)}}, \tag{35}$$

where $\langle\chi\rangle_{\mathscr{G}}$ is the expectation value of the phase fraction $\chi = p/n$. Interestingly we formally obtain (up to the neglected boundary term) the same expression of the zero temperature limit in (17) with the value of χ substituted by its expectation value. Moreover, we can also compute the expectation value of the number of interfaces as

$$\langle i\rangle_{\mathscr{G}} = \frac{\sum_{p=0}^{n}\sum_{i=0}^{n-1}\mathcal{W}_{p,i}\, i\, e^{\Gamma_{p,i}(\sigma)}}{\sum_{p=0}^{n}\sum_{i=0}^{n-1}\mathcal{W}_{p,i}\, e^{\Gamma_{p,i}(\sigma)}}. \tag{36}$$

In Fig. 3 we show the effect of temperature and interfacial energy on the phase transition strategy of the system. Observe that as the surface energy (measured by α) grows (at fixed $\tilde{T}$) the cooperativity increases, whereas the expectation value of the number of interfaces $\langle i\rangle_{\mathscr{G}}$ decreases and the transition is localized more and more around the Maxwell stress $\sigma = 0$. In other words, the behavior is a remnant of the one observed when temperature effects are neglected, as can be seen from Section 3 and from Fig. 3(d) at low values of $\tilde{T}$. On the other hand an opposite regime is obtained when the interfacial energy decreases (smaller values of α). In this case a non cooperative transition may be observed, with a sloped transition plateau and a large number of interfaces. The same effect is attained by increasing the value of the temperature due to the growing importance of the entropic energetic component. Indeed, as we show in the discussion section, in several fundamental physical problems the effective behavior can be influenced by the competition between the entropic and interfacial energy terms.

5. Applied strain: Helmholtz ensemble

To study the system under isometric conditions (assigned displacement, hard device) and evaluate the canonical partition function in the Helmholtz ensemble $\mathscr{H}$, we may observe that it is related to the Gibbs one through a Laplace transform (Manca et al., 2012; Weiner, 1983). In particular, as well known, to switch from Gibbs to Helmholtz ensemble, we evaluate the inverse Laplace transform as a Fourier transform through the change of variable $\sigma \to \imath\omega$. Using the expression of $\mathcal{Z}_{\mathscr{G}}$ in (24) we get

$$\begin{aligned}
\mathcal{Z}_{\mathscr{H}}(\delta) &= \int_{-\infty}^{+\infty} \mathcal{Z}_{\mathscr{G}}(\imath\omega)\, e^{-\tilde{\beta}\imath\omega\delta}\,\mathrm{d}\omega \\
&= \sum_{\{S_j\}} \mathcal{K}_{\mathscr{G}} \int_{-\infty}^{+\infty} e^{\tilde{\beta}\left[\frac{1}{2}\boldsymbol{J}^{-1}(\boldsymbol{m}+(\imath\omega)\mathbf{1})\cdot(\boldsymbol{m}+(\imath\omega)\mathbf{1})-q-\imath\omega\delta\right]}\mathrm{d}\omega \\
&= \sum_{\{S_j\}} \mathcal{K}_{\mathscr{G}}\, e^{\tilde{\beta}\left(\frac{1}{2}\boldsymbol{J}^{-1}\boldsymbol{m}\cdot\boldsymbol{m}-q\right)} \int_{-\infty}^{+\infty} e^{\frac{\tilde{\beta}}{2}\left[-\boldsymbol{J}^{-1}\mathbf{1}\cdot\mathbf{1}\omega^2+2\left(\boldsymbol{J}^{-1}\boldsymbol{m}\cdot\mathbf{1}-\delta\right)\imath\omega\right]}\mathrm{d}\omega \\
&= \sum_{\{S_j\}} \mathcal{K}_{\mathscr{G}}\, e^{\frac{\tilde{\beta}}{2}\left(\boldsymbol{J}^{-1}\boldsymbol{m}\cdot\boldsymbol{m}-2q-\frac{\left(\boldsymbol{J}^{-1}\boldsymbol{m}\cdot\mathbf{1}-\delta\right)^2}{\boldsymbol{J}^{-1}\mathbf{1}\cdot\mathbf{1}}\right)} \int_{-\infty}^{+\infty} e^{-\frac{\tilde{\beta}}{2}\boldsymbol{J}^{-1}\mathbf{1}\cdot\mathbf{1}\left(\omega-\imath\frac{\boldsymbol{J}^{-1}\boldsymbol{m}\cdot\mathbf{1}-\delta}{\boldsymbol{J}^{-1}\mathbf{1}\cdot\mathbf{1}}\right)^2}\mathrm{d}\omega \\
&= \sum_{\{S_j\}} \mathcal{K}_{\mathscr{G}} \sqrt{\frac{2\pi}{\tilde{\beta}\left(\boldsymbol{J}^{-1}\mathbf{1}\cdot\mathbf{1}\right)}}\, e^{\frac{\tilde{\beta}}{2}\left(\boldsymbol{J}^{-1}\boldsymbol{m}\cdot\boldsymbol{m}-2q-\frac{\left(\boldsymbol{J}^{-1}\boldsymbol{m}\cdot\mathbf{1}-\delta\right)^2}{\boldsymbol{J}^{-1}\mathbf{1}\cdot\mathbf{1}}\right)}.
\end{aligned} \tag{37}$$

In the perturbative regime of small α given by (15) and based on the hypothesis in (9) we get

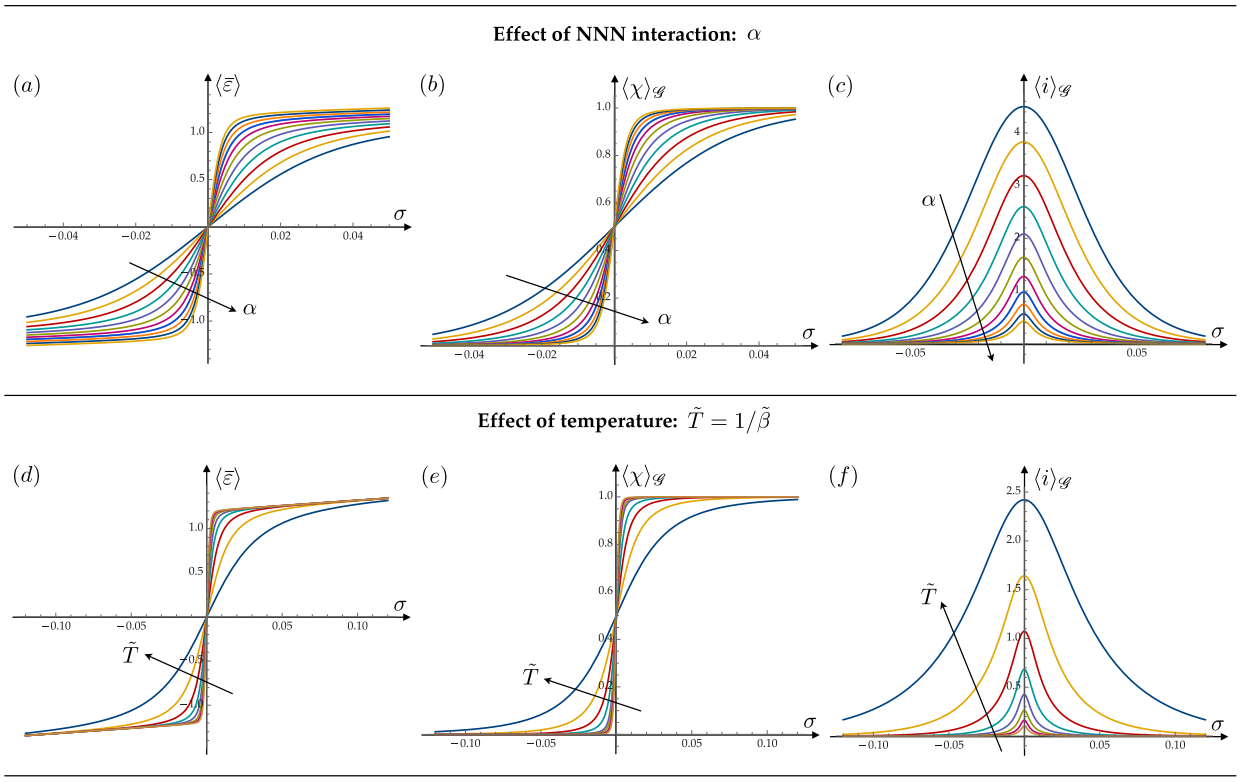

Fig. 3. Gibbs ensemble. Effects of interfacial energy (measured by α) and temperature ($\tilde{T} = 1/\tilde{\beta}$) on the transition behavior. We show the effects of α and $\tilde{T}$ on the stress–strain diagrams in (a) and (d), on the expectation value of the phase fraction χ in (b) and (e) and on the expectation value of the number of interfaces i in (c) and (f), respectively. Parameters: $n = 10$, $\varepsilon_0 = 1$. In the first row $\tilde{\beta} = 30$, $\alpha = 0.0 \to -0.05$ with a step of 0.005. In the second row $\alpha = -0.05$, $\tilde{\beta} = 10 \to 45$ with a step of 5.

$$\mathcal{Z}_{\mathscr{H}}(\delta) \simeq \mathcal{K}_{\mathscr{G}} \sqrt{\frac{2\pi}{\tilde{\beta}(\mathbf{1}\cdot\mathbf{1} - \alpha \boldsymbol{A}\mathbf{1}\cdot\mathbf{1})}} \sum_{\{S_j\}} e^{\frac{\tilde{\beta}}{2}\left(\varepsilon_0^2(\boldsymbol{s}\cdot\boldsymbol{s} - \alpha \boldsymbol{A}\boldsymbol{s}\cdot\boldsymbol{s}) - \frac{(\varepsilon_0 \boldsymbol{s}\cdot\mathbf{1} - \alpha\varepsilon_0 \boldsymbol{A}\boldsymbol{s}\cdot\mathbf{1} - \delta)^2}{\mathbf{1}\cdot\mathbf{1} - \alpha \boldsymbol{A}\mathbf{1}\cdot\mathbf{1}} - n\varepsilon_0^2\right)}. \tag{38}$$

Once more, the exponent of (38) reduces to the equilibrium energy (22) by applying the identities in (16). Following the same reasoning of the Gibbs ensemble we may observe that if we neglect the boundary energy term depending on $S_1 + S_n$ we may express the equilibrium energy as a function of the phase fraction $\chi = p/n$, of the number of interfaces i and of the averaged strain $\bar{\varepsilon} = \delta/n$, so that we obtain

$$\Omega_{p,i}(\bar{\varepsilon}) = -\frac{n\tilde{\beta}}{2}\left\{\frac{\left[(1-4\alpha)(2\,p/n - 1)\varepsilon_0 - \bar{\varepsilon}\right]^2}{1 - \frac{4\alpha}{n}(n-1)} + \frac{4\alpha}{n}\left(n - i - 1\right)\varepsilon_0^2\right\}. \tag{39}$$

Accordingly, the canonical partition function is

$$\mathcal{Z}_{\mathscr{H}}(\bar{\varepsilon}) = \mathcal{K}_{\mathscr{H}} \sum_{p=0}^{n} \sum_{i=0}^{n-1} \mathcal{W}_{p,i}\, e^{\Omega_{p,i}(\varepsilon)}, \tag{40}$$

where

$$\mathcal{K}_{\mathscr{H}} = \mathcal{K}_{\mathscr{G}} \sqrt{\frac{2\pi}{\tilde{\beta}(n - 4\alpha(n-1))}} \tag{41}$$

is a noninfluential constant.

By definition, the Helmholtz free energy is (Manca et al., 2012; Weiner, 1983)

$$\mathcal{F}(\bar{\varepsilon}) = -\frac{1}{\tilde{\beta}} \ln \mathcal{Z}_{\mathscr{H}}(\bar{\varepsilon}), \tag{42}$$

so that the expectation value of the stress, conjugate variable to the displacement $\delta = n\bar{\varepsilon}$, is (Manca et al., 2012; Weiner, 1983)

$$\langle\sigma\rangle = \frac{1}{n}\frac{\partial}{\partial\bar{\varepsilon}}\mathcal{F}(\bar{\varepsilon}) = -\frac{1}{n\tilde{\beta}}\frac{1}{\mathcal{Z}_{\mathscr{H}}(\bar{\varepsilon})}\frac{\partial}{\partial\bar{\varepsilon}}\mathcal{Z}_{\mathscr{H}}(\bar{\varepsilon}), \tag{43}$$

that leads to

$$\langle\sigma\rangle = \frac{1}{1 - \frac{4\alpha}{n}(n-1)}\left[\bar{\varepsilon} - (1-4\alpha)\Big(2\langle\chi\rangle_{\mathscr{H}} - 1\Big)\varepsilon_0\right], \tag{44}$$

where we have introduced the expectation value of the unfolded fraction in the Helmholtz ensemble $\langle\chi\rangle_{\mathscr{H}}$, defined as

$$\langle\chi\rangle_{\mathscr{H}} = \frac{\sum_{p=0}^{n}\sum_{i=0}^{n-1} \mathcal{W}_{p,i}\,\chi\, e^{\Omega_{p,i}(\bar{\varepsilon})}}{\sum_{p=0}^{n}\sum_{i=0}^{n-1} \mathcal{W}_{p,i}\, e^{\Omega_{p,i}(\bar{\varepsilon})}}, \tag{45}$$

with $\chi = p/n$. Thus, also in the case of assigned displacement we obtain formally, up to the neglected boundary term in $S_1 + S_n$, the same expression of the mechanical limit in (21), where we have to consider the expectation value of the phase fraction in (45). The expectation value of the number of interfaces, in the Helmoltz ensemble, using (38), is given by

$$\langle i\rangle_{\mathscr{H}} = \frac{\sum_{p=0}^{n}\sum_{i=0}^{n-1} \mathcal{W}_{p,i}\, i\, e^{\Omega_{p,i}(\bar{\varepsilon})}}{\sum_{p=0}^{n}\sum_{i=0}^{n-1} \mathcal{W}_{p,i}\, e^{\Omega_{p,i}(\bar{\varepsilon})}}, \tag{46}$$

The effect of temperature and interface energy in the case of assigned displacement is described in Fig. 4. As in the isotensional setting, the influence of temperature and interfacial energy terms affect the cooperativity, that increases as α grows and T decreases. The main differences between isotensional and isometric boundary conditions reflect the discussion anticipated in the mechanical case in Section 3. Accordingly, in the case of assigned displacement, the minimum expected value of interfaces, attained for larger values of α and low values of $\tilde{T}$ during phase

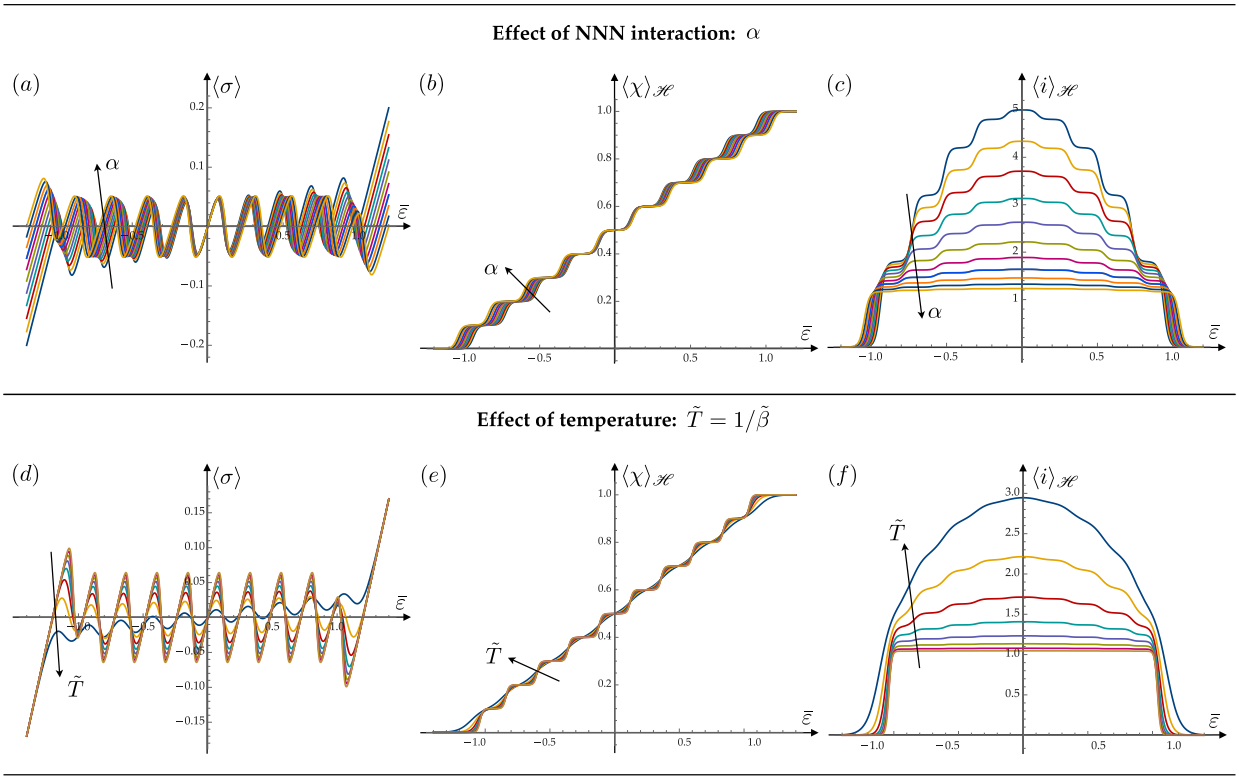

Fig. 4. Helmholtz ensemble. In the first row we show the effect of α and in the second row the effect of $\tilde{T}$. In (a) and (c) we the stress-strain curves are represented, in (b) and (e) the expectation value of $\langle\chi\rangle_{\mathscr{H}}$ and in (c) and (f) the expectation value of $\langle i\rangle_{\mathscr{H}}$. Parameters: $n = 10$, $\varepsilon_0 = 1$. In the first row $\tilde{\beta} = 30$ and $\alpha = 0.0 \to -0.05$ with a step of 0.005. In the second row $\alpha = -0.05$ and $\tilde{\beta} = 10 \to 45$ with a step of 5.

nucleation is $\langle i\rangle_{\mathscr{H}} = 1$. Moreover, the transition corresponds to sawtooth stress-strain diagrams. As Fig. 4(a) and (c) shows, due to the presence of non local energy terms, the nucleation and propagation stresses may differ considerably. Observe that also the size of the first nucleated domain may be, when entropic effects are considerd, significantly regulated by both parameters.

More in detail, in Fig. 5 we show how fundamental aspects such as the different nucleation and propagation stresses and the size of the initial nucleation domain are affected by variable interfacial energy, temperature, and discreteness size. In particular, the nucleation peak is strongly influenced by all these parameters and we observe that larger values are obtained for high values of α and low values of temperature. On the other hand, the size of the first nucleated domain grows as α increases and $\tilde{T}$ decreases. Another important effect is that by increasing temperature the stress-strain diagrams attains a 'wiggly' shape instead of 'sawtooth', as shown in Fig. 5(c). It is important to remark that these diagrams represent expectation values and are a counterpart of the process of switching, due to temperature effects, between solutions with similar energy. Moreover, as the temperature grows we may observe the transition from a constant average of the transition stress plateaux to a sloped one. This behavior is limited by the presence of non-local terms, as shown in Fig. 5(b). The effect of discreteness is described in Fig. 5(a) that shows decreasing values of the peak and increasing number of nucleated elements as n increases.

6. Comparison with Molecular Dynamics

In order to test the effectiveness of the proposed model in deducing the transition behavior taking into account the role of interfacial energy and temperature effects, we compare our theoretical results with numerical experiments based on Molecular Dynamics (MD) of shape memory nanowires (NWs). These systems acquired large attention due their incredible properties in terms of energy storage (no hysteresis), large actuation strain (> 30% as compared to $\sim$ 5% of the bulk ones) and stress (> 3 GPa as compared to $\sim$ 0.5GPa of the bulk ones) (Li et al., 2010). Several MD simulations, also supported by experimental tests (see *e.g.* Refs. Ma et al., 2013; Seo et al., 2013), showed that such superior behavior results from a different mechanism of microstructure evolution during the phase transition. Indeed, in SMA nanowires the phase transition process is accompanied by a shear dominant diffusionless transformation, leading to the formation and the migration of defect-free twins connecting the two (kinematically incompatible) phases. The typical applications are based on face-centered cubic (FCC) metallic (Cu, Ni, Au and Ag) nanowires whose transition is simply accompanied by a crystal reorientation enabled by the notion of coherent twin boundaries. This leads to a different type of pseudoelasticity, as compared to bulk materials, that is not regulated by martensitic phase transition, but by the propagation of twins leading to crystal reorientations (Liang et al., 2007). As a result, the same bulk materials do not show a pseudoelastic behavior. The energetic competition between dislocation and twinning nucleation at a crack tip has also been described in bulk materials (Tadmor and Hai, 2003). In the case of nanowires, coherent twin interfaces are formed between the two phases that then propagates along the wire axis when the average strain is increased. More detailed metallographic analysis on the underlying mechanism of twin regulated deformation in nanowires can be found *e.g.* in Ref. Park et al. (2006). This process is reversible and it is responsible of the incredible pseudoelastic behavior observed in these materials.

We begin by testing our model in predicting the behavior obtained in the simulations performed on Ni-Co alloy nanowires in Ref. Lu et al. (2019). Some remarks are in order. As previously stated, our model is one-dimensional. On the other hand, as we deduce qualitatively in the following, the role of the lateral size of the system can be related to

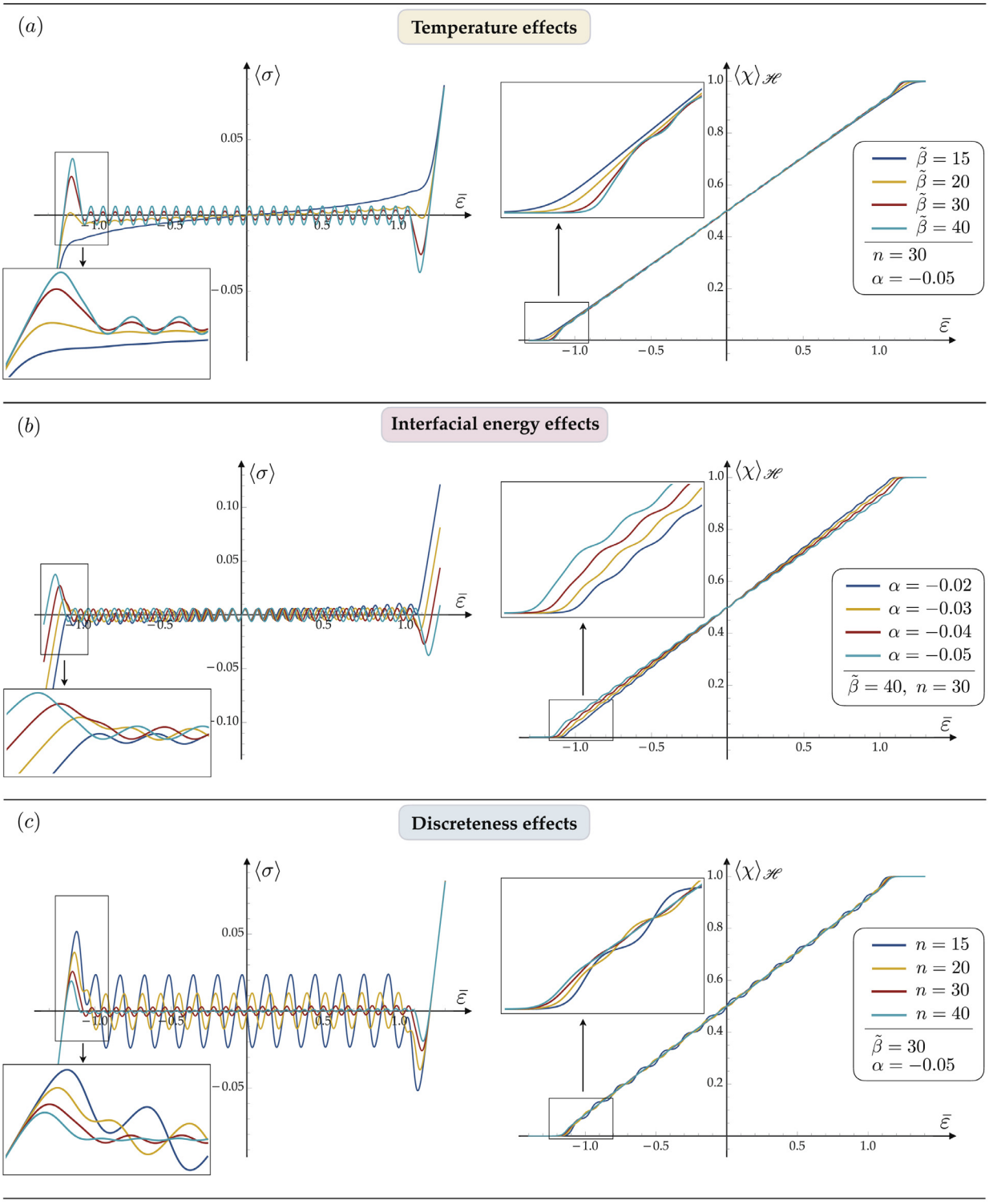

Fig. 5. Nucleation of the first phase in the Helmholtz ensemble. In the first row the effect of the increasing n is shown. In the second row the effect of the strength of the non local interactions is displayed. In the third row the effect of the temperature is represented. Parameter on the legends.

the strength of non local interactions included in our model, but also in the presence of non local interactions with the loading device. Moreover, it is important to stress that physical constitutive parameters of the system such as the Young modulus depend on both temperature and lateral size. This dependence is here used to fit the numerical results in MD. Among many effects such as the presence of Co in the alloy and the role of surface/internal defects, in Ref. Lu et al. (2019) the authors study the temperature dependence of the stress behavior. They simulate a nanowire with dimensions $2.465\text{nm} \times 2.464\text{nm} \times 19.712\text{nm}$. In order to adapt this system to our one-dimensional model, we consider a unit reference length l equal to the lattice constant $l = a_{Ni} = 0.3499$ nm (for Nickel) and, therefore, $n = 55$ oscillators in our formulas. It is important

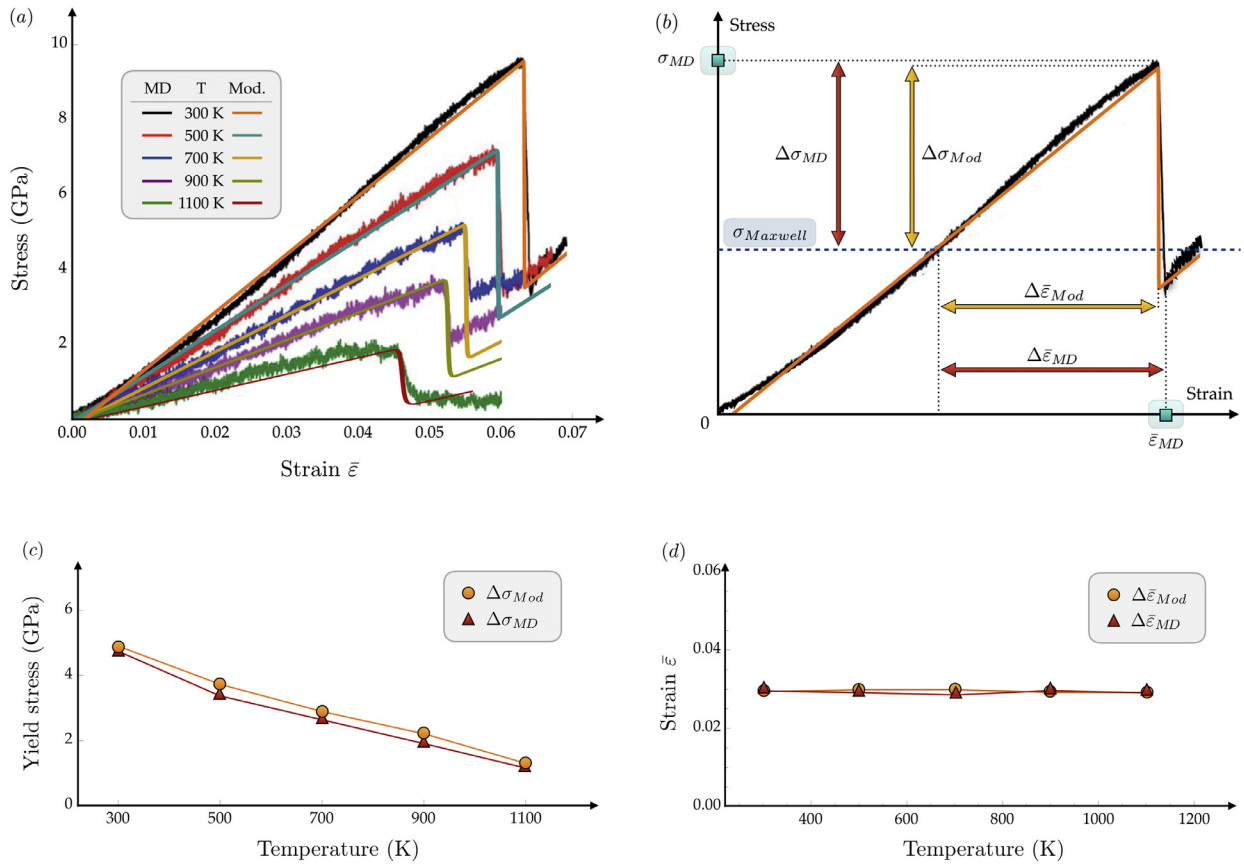

Fig. 6. Comparison of results obtained from the model presented in the paper those from Molecular Dynamics (MD) simulations. Simulation adapted from Ref. (Lu et al., 2019), published by the Royal Society of Chemistry. Details about the values of the parameters can be found in the main text. (a): Stress–strain curves. (b): relevant quantities used for the comparison in panel (c) and (d), see main text for details. (c) dependence of the yield stress on temperature. (d) Dependence on temperature of the strain corresponding to the drop of the yield stress.

to observe that *in order to calibrate the system and fit the experimental data we have only two parameters to be fixed: α and ε_0*. Here we set the value of the reference strain of the second phase $\varepsilon_0 = 0.18$ and $\alpha = -0.2$. The values of the modulus E are the ones proposed in Lu et al. (2019) and accordingly we deduce $k = EA$ (with A the section considered in Lu et al. (2019)). Similarly, given the temperatures, we may deduce the corresponding values of $\tilde{\beta} = \beta k l$.

The comparison of the theoretical and numerical results are exibited in Fig. 6(a), where the stress-strain curves for different values of the temperature are represented. In particular, using Eq. (44) we obtain that $E(1 - 4\alpha(n-1)/n)\langle\sigma\rangle$ corresponds to the stress measured in the MD simulations. We may observe that, despite the oversimplification of the model, the theoretical response is in a very good agreement with the MD simulations. We remark that although we may observe that for $T = 500, 700, 900$ K the description of the size of the first stress drop is not accurate, the authors show in the paper that effects such as internal defects and the percentage of diluted Cobalt can be responsible for this effect. On the other hand, as shown Fig. 5(c) this value differs from the physically meaningful difference of the nucleation and propagation stress (not reported by the authors), because it strictly depends on the precise position of the first drop.

In order to obtain a more clear comparison with the MD results, in Fig. 6(c) and (d) we extracted the values of the nucleation stresses and strains depending on temperature. It is important to remark that in our model we assumed for simplicity of notation a zero Maxwell stress. To reconcile the theoretical results and the MD experiments, in Fig. 6(b) we show how we deduce the value of the propagation (Maxwell) stress and the corresponding strain. The agreement between the MD results (red triangles) and those obtained from the model (orange circles) is excellent in both cases.

We have also tested our model to verify the possibility of describing the fundamental size effects observed in shape memory nanowires, showing an increasing role of the interface energy as the size of the specimen decreases. In particular, we analyzed the size effect on the nucleation (yield) stress studied in Ref. Wu (2006). There, the author performed MD simulations considering Cu nanowires with fixed aspect ratio 1:1:3 ($\gamma = L_s/b_s = 3$ in Fig. 7(a)) and variable lateral size. Following the same procedure described above, with the aim of fitting the MD results, we have fixed the reference length l with the value of Copper lattice constant $l = a_{Cu} = 0.3609$ nm, temperature $T = 1$K (as indicated in the paper) and $\varepsilon_0 = 0.23$. Thus, we need to consider a variable number of elements $n \simeq L_s/l$ ranging from 14 to 77 where L_s is the length of the sample considered in Ref. Wu (2006). Another important feature to point out is that the (effective) elastic modulus depends on the lateral size $E = E(b_s)$. This dependence is reported in the paper (Wu, 2006) and is used in our computation to evaluate the stiffness $k = k(b_s) = E(b_s)b_s^2$.

To evaluate how the change of length influences the parameter α we may, in a first approximation, consider the following energy rescaling reasoning. A rough estimate of the total energy density of the MD system can be obtained, separating the contribution of bulk and surface energy, as follows:

$$\Phi_{tot}^{MD} = \Phi_b^{MD} + \Phi_s^{MD} = \frac{E(b_s)\gamma b_s^3 + C b_s^2}{\gamma b_s^3} = E(b_s) + \frac{C}{\gamma b_s}, \tag{47}$$

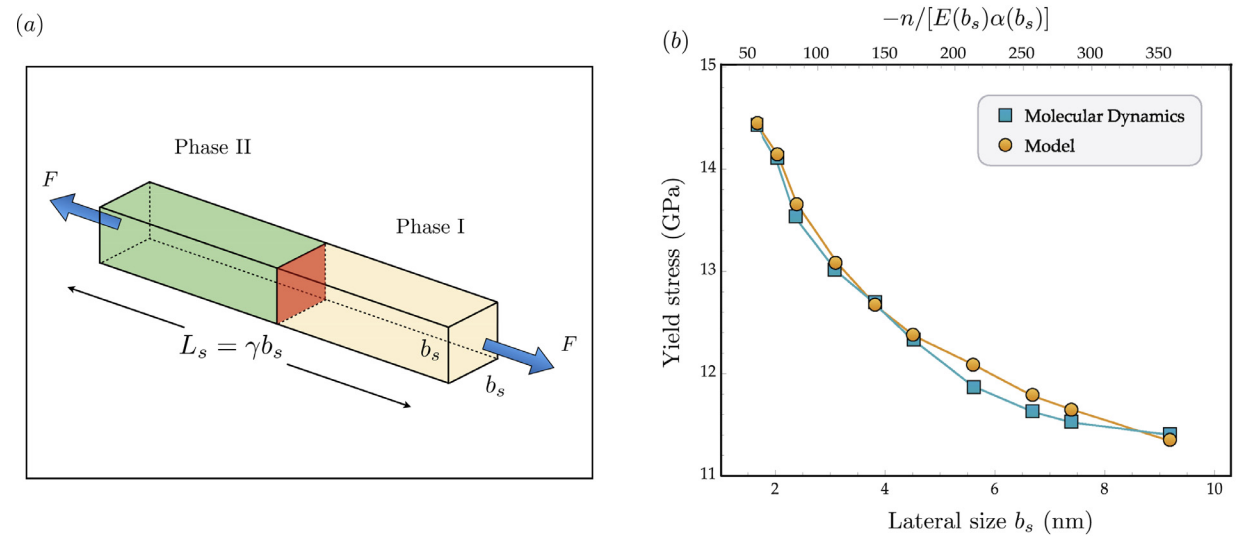

Fig. 7. (a) One dimensional scheme of the shape memory wires. (b) Dependence of the nucleation (yield) stress on the lateral size b_s (MD simulations reproduced from Wu (2006)) and theoretical model (see the text for the deduction of the parameters from the MD experiments).

where C is the surface energy constant. In particular we have that the relative role of the surface energy is

$$\xi^{MD} := \frac{\Phi_s^{MD}}{\Phi_b^{MD}} = \frac{C}{E(b_s)\gamma b_s}. \tag{48}$$

On the other hand, in the proposed model we have that the analogous quantities are given by

$$\Phi_{tot}^{Mod} = \Phi_b^{Mod} + \Phi_s^{Mod} = \frac{k(b_s)nl + \alpha k(b_s)l}{nlb_s^2} = E(b_s) + E(b_s)\frac{\alpha}{n}, \tag{49}$$

so that

$$\xi^{Mod} := \frac{\Phi_s^{Mod}}{\Phi_b^{Mod}} = \frac{\alpha(b_s)}{n}. \tag{50}$$

We obtain then the main assumption for the comparison of molecular dynamic and model rescaling effects by comparing (48) and (50) that gives $\frac{\alpha(b_s)}{n} \sim \frac{1}{E(b_s)b_s}$, and since $b_s = \gamma L_s \propto n$, we get

$$\alpha(b_s) \sim \frac{1}{E(b_s)}. \tag{51}$$

The behavior resulting from this rescaling is reproduced in Fig. 7(b) where according with the assumption (51) the parameter α ranges in the interval $\alpha \in (-0.25, -0.215)$. Observe that again we have two only parameters to fit the experimental data, *i.e.* the value of ϵ_0 and the value of the constant of proportionality in (51). Again, despite the simplification of the model, we obtain a very satisfying agreement.

7. Discussion and conclusions

We derived a fully analytical approach to describe the competition of entropic and interfacial energy terms in the transition strategy of a bistable material. More specifically, we considered a prototypical system constituted by a lattice of bistable elements and non local NNN interactions with a concave energy density reproducing the presence of an interfacial energy term penalizing the formation of new interfaces. The extension to the opposite case of NNN terms with convex energy, playing the (antiferromagnetic) role of favoring the presence of interfaces is straightforward in our framework, but not explicitly discussed and applied in this work. The presence of this energetic term plays an important role leading in the case of isometric loading to the presence of an initial stress-peak distinguishing the nucleation and propagation stresses. Roughly speaking, due to the presence of interfacial energy terms, the transition from a homogeneous reference phase to a two phase configuration is delayed because of the energetically unfavorable event of nucleation of a new phase and the formation of interfaces. All these features are observed in different phase transition materials, some of which are explicitly discussed in this section. On the other hand, the presence of interfacial energy terms, in the absence of temperature effect or other non local interactions terms would lead to the possibility of one single interface. The experimental behavior contradicts this result and this effect may be ascribed to several different phenomena such as interaction with the loading device (Puglisi, 2006; 2007; Ren and Truskinovsky, 2000), compatibility and dynamical effects (Abeyaratne et al., 1996; Müller, 1999), inhomogeneities and rate effects (Shaw and Kyriakides, 1997) and temperature effects as considered in this paper.

Specifically, we have introduced a model whose behavior is of interest in the physical cases where there are competing energy terms, namely in situations where non-local interaction effects are of the same order of magnitude of temperature driven entropic effects, such as in nanowires or several biological materials discussed in the following. In this cases the system behavior has to be described in the framework of Equilibrium Statistical Mechanics. Hence, we are able to analytically describe the effect of temperature, at least in the rate-independent regime. The extension to include rate effects can be attained by considering classical barrier dependent behaviors, as reported *e.g.* in Ref. Benichou and Givli (2013).

The results of the model have been summarized in Fig. 8. Observe that the behavior of the system when entropic energy terms can be neglected, coinciding with the system studied in Section 3 in the limit of $\tilde{T} = 1/\tilde{\beta} \to 0$, is represented in the first row of Fig. 8 with the $\star$ symbol. The figure shows the fundamental role that may be played by entropic effects. In particular, the size of the first nucleated domain is essentially temperature independent but, on the other hand, it strongly depends on the interfacial energy. On the other hand, both the stress peak and the number of interfaces may strongly depend on temperature. In particular, we may observe that the stress peak decreases as temperature grows whereas the cooperativity decreases, with an increasing number of maximum number of interfaces. This is an expected result, because by increasing the temperature the solution characterized by a high values of the entropy –here measured by the number (26) of permutations corresponding to the same values of p and i– are energetically favored. In these cases we may interpret the experimental observation of less cooperative transition as induced by temperature entropic effects.

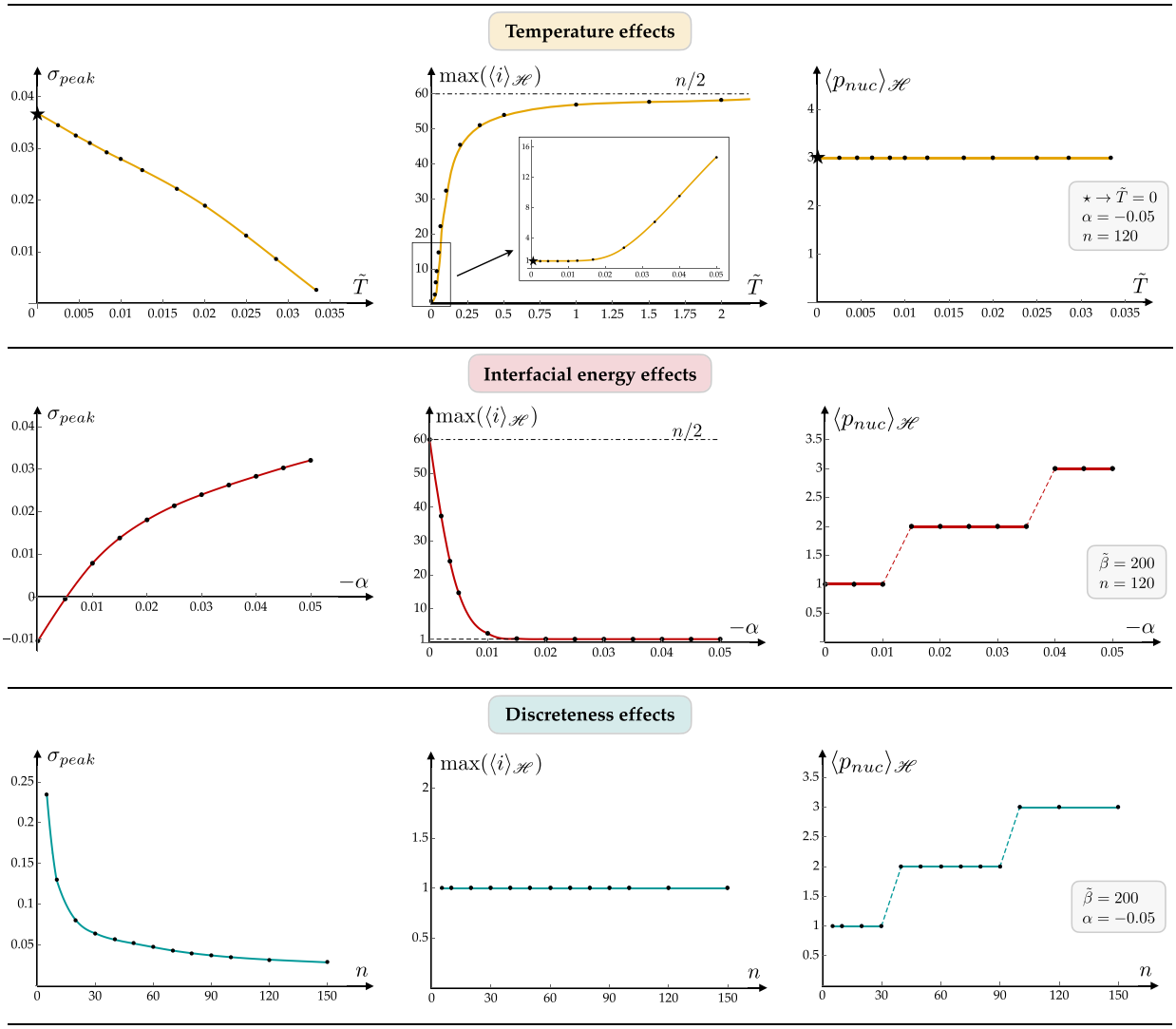

Fig. 8. Synthetic description of the analytical results. We show the influence of the temperature T (top), of the interfacial energy parameter α (middle) and of the discrete parameter n (bottom) on the transition behavior in terms of nucleation peak (left), maximum number of interfaces (center) and size of the nucleated domain (right). In the first row we indicate with $\star$ the behavior of the system in Section 3 coinciding with the limit of $\tilde{T} \to 0$ when entropic effects can be neglected.

As discussed in Section 6, our model can be considered as a prototype for the analysis of the temperature and size dependent transition behavior of SMA nanowires. The main reason of the different behavior of SMA nanowires as compared with bulk materials is due to the well known important role of surface energy terms as compared with the bulk one as the scale of the specimens decreases. Specifically, two different scale effects have to be considered (Seo et al., 2013). The first one corresponds to the energy of the wire surface that regulates, together with the bulk energy, the (diameter dependent) effective energy of the phases. As a result, the energy wells and, in particular, the Maxwell stress corresponding to the propagation threshold, are scale-dependent parameters. Of course, since our model considers global energy minimizers only, we neglect hysteretic effects, but this is in agreement with the typical behavior of nanowires that often are characterized by a reversible (Lao et al., 2013) transition. On the other hand, extensions to consider local energy minimizers can be considered (Benichou and Givli, 2013; Puglisi and Truskinovsky, 2005) (see also the low scale interpretation in Ref. Liang et al. (2007) of possible dissipation associated with the discrete process of twin propagation). The second surface energy term, important at these scales, is the interfacial energy associated with the formation of a twin, here measured by non-local energy terms through the parameter α. While the size dependence of this energy can be theoretically estimated depending on the specific twin connecting the two phases (Zhang et al., 2008), in Section 6 we deduced this dependence in our one dimensional setting by simple scaling arguments. When the size of the wire is fixed and the temperature is changed, we expect that the bulk energy of the wires does not change whereas the nucleation stress can be influenced by temperature effects as measured by our model. This is reflected by a variation of both the nucleation and propagation stress with the size of the wire (both α and the energy wells are modified), whereas temperature only influences the nucleation stress (see Fig. 6). Such behavior, reproduced from our model, is reflected in different papers based on MD simulations (Lao et al., 2013; Seo et al., 2011). Moreover, as suggested by our model, the possibility of more twins formations has been described in several contributions (Guo et al., 2009; Rezaei and Deng, 2017). Interestingly, as predicted from our results, the experimental behavior (Guo et al., 2009) shows that also the number of interfaces is influenced by temperature with a 'Bell type' growth as described in Fig. 4(c) and (f). We then considered explicitly the possibility of describing the dependence of the nucleation and propagation stresses

from the wire diameter. In this case, as described above, also the bulk energy depends from the size and can be deduced from MD experiments. Once the corresponding rescaling quantities are adopted in our model, we showed the possibility of well describing the size dependent transition behavior (see Fig. 7).

A second important field of application for the results of our model that we would like just to sketch in this paper and that will be the subject of our future work is related to the important role that interdomains interactions can play in the stability and cooperativity transition of multidomain proteins, undergoing a conformational folded → unfolded transition, as compared with the stability of isolated domains (Bhaskara and Srinivasan, 2011; Law et al., 2003; Xu et al., 2013). This subject has achieved in recent years increasing attention after a long period when research was focussed only on single domains behavior both experimentally and theoretically (see Refs. Bhaskara and Srinivasan, 2011; Law et al., 2003; Xu et al., 2013 and references therein). In this second field, the possibility of describing important experimental effects in the framework of Statistical Mechanics with non convex energies have been shown in Refs. Bellino et al. (2019); De Tommasi et al. (2013); Florio and Puglisi (2019); Giordano (2017); Manca et al. (2013). In these papers the two wells correspond to the folded and unfolded states. On the other hand, in these models, no NNN interactions were considered. Experimental and theoretical literature showed the important role of interdomain interactions in the unfolding behavior of proteins and their possible roles in the insurgence of diseases (Bhaskara and Srinivasan, 2011). A typical well known example is the stabilization effect in spectrin repeat unfolding. Thermal stability analysis clearly show the important stabilization effects (MacDonald and Pozharski, 2001) due to non local interactions between different two-states domains. Single molecule force spectroscopy shows that this effect can induce a contemporary transition of two domains at the first stress peak (Rief et al., 1999). Interestingly, as theoretically deduced with our model, cooperativity is lost if temperature is increased (Batey et al., 2005). Moreover, a similar behavior has been observed in Filamin A proteins, where domain-domain interactions lead to a hierarchy of unfolding forces that may be properly studied by nonlocal models (Xu et al., 2013). A recent modeling approach of these macromolecular behaviors is based on an Ising scheme suitably coupled with the chain of bistable units representing the protein domains (Benedito and Giordano, 2018a). Our results show the possibility of modeling such behavior in the framework of Statistical Mechanics based on the consideration of non local interactions. In particular, beyond the possibility of the contemporary transition of domains, the model shows that cooperativity can be increased by the effect of NNN interactions whereas it can be hided by entropic effects when temperature increases. It is important anyway to remark that other important effects, such as allosteric effects of binding sites and fully non local interactions in the tertiary and quaternary structures cannot be described in the simple one dimensional setting here considered (Daily and Gray, 2009). More detailed analysis and comparison with MD tests and actual experiments will be considered in future works.

Declaration of Competing Interest

The authors declare that they have no known competing financial interests or personal relationships that could have appeared to influence the work reported in this paper.

Acknowledgments

SG acknowledges the region “Hauts de France” for the financial support under project MEPOFIB. LB, GF and GP have been supported by the Italian Ministry MIUR-PRIN project “Mathematics of active materials: From mechanobiology to smart devices”. LB, GF and GP are supported by GNFM (INdAM). GP and GF by the Italian Ministry MISE through the project RAEE SUD-PVP. GF is also supported by INFN through the project “QUANTUM”, by the FFABR research grant (MIUR) and the PON S.I.ADD.

References

Abeyaratne, R., Chu, C., James, R.D., 1996. Kinetics of materials with wiggly energies: theory and application to the evolution of twinning microstructures in a cu-al-ni shape memory alloy. Philoso. Mag. A 73 (2), 457–497. doi:10.1080/01418619608244394.

Allen, S.M., Cahn, J.W., 1979. A microscopic theory for antiphase boundary motion and its application to antiphase domain coarsening. Acta Metall. 27 (6), 1085–1095. doi:10.1016/0001-6160(79)90196-2.

Angenent, S., Gurtin, M.E., 1989. Multiphase thermomechanics with interfacial structure 2. Evolution of an isothermal interface. Arch. Rat. Mech. Anal. 108 (3), 323–391. doi:10.1007/BF01041068.

Ball, J.M., James, R.D., 1989. Fine phase mixtures as minimizers of energy. In: Analysis and Continuum Mechanics. Springer, pp. 647–686. doi:10.1007/BF00281246.

Batey, S., Randles, L.G., Steward, A., Clarke, J., 2005. Cooperative folding in a multidomain protein. J. Mol. Biol. 349 (5), 1045–1059. doi:10.1016/j.jmb.2005.04.028.

Bellino, L., Florio, G., Puglisi, G., 2019. The influence of device handles in single-molecule experiments. Soft Matter 15 (43), 8680–8690. doi:10.1039/C9SM01376H.

Benedito, M., Giordano, S., 2018. Isotensional and isometric force-extension response of chains with bistable units and ising interactions. Phys. Rev. E 98 (5), 052146. doi:10.1103/PhysRevE.98.052146.

Benedito, M., Giordano, S., 2018. Thermodynamics of small systems with conformational transitions: the case of two-state freely jointed chains with extensible units. J. Chem. Phys. 149 (5), 054901. doi:10.1063/1.5026386.

Benedito, M., Giordano, S., 2020. Unfolding pathway and its identifiability in heterogeneous chains of bistable units. Phys. Lett. A 384 (5), 126124. doi:10.1016/j.physleta.2019.126124.

Benichou, I., Givli, S., 2013. Structures undergoing discrete phase transformation. J. Mech. Phys. Solids 61 (1), 94–113. doi:10.1016/j.jmps.2012.08.009.

Bhaskara, R.M., Srinivasan, N., 2011. Stability of domain structures in multi-domain proteins. Sci. Rep. 1, 40. doi:10.1038/srep00040.

Bilal, O.R., Foehr, A., Daraio, C., 2017. Bistable metamaterial for switching and cascading elastic vibrations. Proc. Natl. Acad. Sci. USA 114 (18), 4603–4606. doi:10.1073/pnas.1618314114.

Carr, J., Gurtin, M.E., Slemrod, M., 1984. Structured phase transitions on a finite interval. Technical Report. Carnegie-Mellon Inst. Resear. Pittsburgh PA doi:10.1007/BF00280031.

Coleman, B.D., 1983. Necking and drawing in polymeric fibers under tension. Arch. Rat. Mech. Anal. 83 (2), 115–137. doi:10.1007/BF00282158.

Daily, M.D., Gray, J.J., 2009. Allosteric communication occurs via networks of tertiary and quaternary motions in proteins. PLoS Comput. Biol. 5 (2). doi:10.1371/journal.pcbi.1000293.

De Tommasi, D., Millardi, N., Puglisi, G., Saccomandi, G., 2013. An energetic model for macromolecules unfolding in stretching experiments. J. R. Soc. Interface 10 (88), 20130651. doi:10.1098/rsif.2013.0651.

De Tommasi, D., Puglisi, G., Saccomandi, G., 2015. Multiscale mechanics of macromolecular materials with unfolding domains. J. Mech. Phys. Solids 78, 154–172. doi:10.1016/j.jmps.2015.02.002.

Denisov, S.I., Hänggi, P., 2005. Domain statistics in a finite Ising chain. Phys. Rev. E 71 (4), 046137. doi:10.1103/PhysRevE.71.046137.

Efendiev, Y.R., Truskinovsky, L., 2010. Thermalization of a driven bi-stable FPU chain. Continuum Mech. Thermodyn. 22 (6-8), 679–698. doi:10.1007/s00161-010-0166-5.

Ericksen, J.L., 1975. Equilibrium of bars. J. Elast. 5 (3–4), 191–201. doi:10.1007/BF00126984.

Fedelich, B., Zanzotto, G., 1992. Hysteresis in discrete systems of possibly interacting elements with a double-well energy. J. Nonlinear Sci. 2, 319–342. doi:10.1007/BF01208928.

Florio, G., Puglisi, G., 2019. Unveiling the influence of device stiffness in single macromolecule unfolding. Sci. Rep. 9 (1), 1–11. doi:10.1038/s41598-019-41330-x.

Florio, G., Puglisi, G., Giordano, S., 2020. On the role of temperature in the decohesion of an elastic chain tethered to a substrate by on-site breakable link. Phys. Rev. Res. In press.

Giordano, S., 2017. Spin variable approach for the statistical mechanics of folding and unfolding chains. Soft Matter 13 (38), 6877–6893. doi:10.1039/C7SM00882A.

Giordano, S., 2018. Helmholtz and Gibbs ensembles, thermodynamic limit and bistability in polymer lattice models. Contin. Mech. Thermodyn. 30, 459–483. doi:10.1007/s00161-017-0615-5.

Guo, X., Liang, W., Zhou, M., 2009. Mechanism for the pseudoelastic behavior of FCC shape memory nanowires. Exp. Mech. 49 (2), 183–190. doi:10.1007/s11340-008-9173-x.

Ising, E., 1925. Beitrag zur theorie des ferromagnetismus. Z. Phys. 31 (1), 253–258. doi:10.1007/BF02980577.

Keller, A., Cheng, S.Z., 1998. The role of metastability in polymer phase transitions. Polymer 39 (19), 4461–4487. doi:10.1016/S0032-3861(97)10320-2.

Khachaturyan, A.G., 1983. Theory of Structural Transformations in Solids. John Wiley & Sons.

Lao, J., Tam, M.N., Pinisetty, D., Gupta, N., 2013. Molecular dynamics simulation of FCC metallic nanowires: a review. Jom 65 (2), 175–184. doi:10.1007/s11837-012-0465-3.

Law, R., Carl, P., Harper, S., Dalhaimer, P., Speicher, D.W., Discher, D.E., 2003. Cooperativity in forced unfolding of tandem spectrin repeats. Biophys. J. 84 (1), 533–544. doi:10.1016/S0006-3495(03)74872-3.

Li, S., Ding, X., Li, J., Ren, X., Sun, J., Ma, E., 2010. High-efficiency mechanical energy storage and retrieval using interfaces in nanowires. Nano Lett. 10 (5), 1774–1779. doi:10.1021/nl100263p.

Liang, W., Srolovitz, D.J., Zhou, M., 2007. A micromechanical continuum model for the tensile behavior of shape memory metal nanowires. J. Mech. Phys. Solids 55 (8), 1729–1761. doi:10.1016/j.jmps.2007.01.001.

Lu, X., Yang, P., Luo, J., Ren, J., Xue, H., Ding, Y., 2019. Tensile mechanical performance of Ni–Co alloy nanowires by molecular dynamics simulation. RSC Adv. 9 (44), 25817–25828. doi:10.1039/C9RA04294F.

Ma, F., Xu, K.-W., Chu, P.K., 2013. Surface-induced structural transformation in nanowires. Mater. Sci. Eng.: R: Rep. 74 (6), 173–209. doi:10.1016/j.mser.2013.05.001.

MacDonald, R.I., Pozharski, E.V., 2001. Free energies of urea and of thermal unfolding show that two tandem repeats of spectrin are thermodynamically more stable than a single repeat. Biochemistry 40 (13), 3974–3984. doi:10.1021/bi0025159.

Makarov, D.E., 2009. A theoretical model for the mechanical unfolding of repeat proteins. Biophys. J. 96 (6), 2160–2167. doi:10.1016/j.bpj.2008.12.3899.

Manca, F., Giordano, S., Palla, P.L., Cleri, F., Colombo, L., 2013. Two-state theory of single-molecule stretching experiments. Phys. Rev. E 88 (3), 032705. doi:10.1103/PhysRevE.87.032705.

Manca, F., Giordano, S., Palla, P.L., Zucca, R., Cleri, F., Colombo, L., 2012. Elasticity of flexible and semiflexible polymers with extensible bonds in the Gibbs and Helmholtz ensembles. J. Chem. Phys. 136 (15), 154906. doi:10.1063/1.4704607.

Müller, I., Seelecke, S., 2001. Thermodynamic aspects of shape memory alloys. Math. Comput. Model. 34 (12-13), 1307–1355. doi:10.1016/S0895-7177(01)00134-0.

Müller, I., Villaggio, P., 1977. A model for an elastic-plastic body. Arch. Rat. Mech. Anal. 65 (1), 25–46. doi:10.1007/BF00289355.

Müller, S., 1999. Variational models for microstructure and phase transitions. In: Calculus of Variations and Geometric Evolution Problems. Springer, pp. 85–210. doi:10.1007/BFb0092670.

Park, H.S., Gall, K., Zimmerman, J.A., 2006. Deformation of FCC nanowires by twinning and slip. J. Mech. Phys. Solids 54 (9), 1862–1881. doi:10.1016/j.jmps.2006.03.006.

Peyrard, M., 2004. Nonlinear dynamics and statistical physics of DNA. Nonlinearity 17 (2), R1. doi:10.1088/0951-7715/17/2/R01.

Puglisi, G., 2006. Hysteresis in multi-stable lattices with non-local interactions. J. Mech. Phys. Solids 54 (10), 2060–2088. doi:10.1016/j.jmps.2006.04.006.

Puglisi, G., 2007. Nucleation and phase propagation in a multistable lattice with weak nonlocal interactions. Contin. Mech. Thermodyn. 19 (5), 299–319. doi:10.1007/s00161-007-0056-7.

Puglisi, G., De Tommasi, D., Pantano, M., Pugno, N., Saccomandi, G., 2017. Micromechanical model for protein materials: from macromolecules to macroscopic fibers. Phys. Rev. E 96 (4), 042407. doi:10.1103/PhysRevE.96.042407.

Puglisi, G., Truskinovsky, L., 2000. Mechanics of a discrete chain with bi-stable elements. J. Mech. Phys. Solids 48 (1), 1–27. doi:10.1016/S0022-5096(99)00006-X.

Puglisi, G., Truskinovsky, L., 2002. Rate independent hysteresis in a bi-stable chain. J. Mech. Phys. Solids 50 (2), 165–187. doi:10.1016/S0022-5096(01)00055-2.

Puglisi, G., Truskinovsky, L., 2005. Thermodynamics of rate-independent plasticity. J. Mech. Phys. Solids 53 (3), 655–679. doi:10.1016/j.jmps.2004.08.004.

Puglisi, G., Truskinovsky, L., 2013. Cohesion-decohesion asymmetry in geckos. Phys. Rev. E 87 (3), 032714. doi:10.1103/PhysRevE.87.032714.

Ren, X., Truskinovsky, L., 2000. Finite scale microstructures in nonlocal elasticity. J. Elast. Phys. Sci. Solids 59 (1–3), 319–355. doi:10.1023/A:1011003321453.

Rezaei, R., Deng, C., 2017. Pseudoelasticity and shape memory effects in cylindrical FCC metal nanowires. Acta Mater. 132, 49–56. doi:10.1016/j.actamat.2017.04.039.

Rief, M., Pascual, J., Saraste, M., Gaub, H.E., 1999. Single molecule force spectroscopy of spectrin repeats: low unfolding forces in helix bundles. J. Mol. Biol. 286 (2), 553–561. doi:10.1006/jmbi.1998.2466.

Seo, J.-H., Park, H.S., Yoo, Y., Seong, T.-Y., Li, J., Ahn, J.-P., Kim, B., Choi, I.-S., 2013. Origin of size dependency in coherent-twin-propagation-mediated tensile deformation of noble metal nanowires. Nano Lett. 13 (11), 5112–5116. doi:10.1021/nl402282n.

Seo, J.-H., Yoo, Y., Park, N.-Y., Yoon, S.-W., Lee, H., Han, S., Lee, S.-W., Seong, T.-Y., Lee, S.-C., Lee, K.-B., et al., 2011. Superplastic deformation of defect-free Au nanowires via coherent twin propagation. Nano Lett. 11 (8), 3499–3502. doi:10.1021/nl2022306.

Seth, S., 2016. Combinatorial approach to exactly solve the 1D Ising model. Eur. J. Phys. 38 (1), 015104. doi:10.1088/1361-6404/38/1/015104.

Shang, X., Liu, L., Rafsanjani, A., Pasini, D., 2018. Durable bistable auxetics made of rigid solids. J. Mater. Res. 33 (3), 300–308. doi:10.1557/jmr.2017.417.

Shaw, J.A., Kyriakides, S., 1997. On the nucleation and propagation of phase transformation fronts in a NiTi alloy. Acta Mater. 45 (2), 683–700. doi:10.1016/S1359-6454(96)00189-9.

Tadmor, E., Hai, S., 2003. A Peierls criterion for the onset of deformation twinning at a crack tip. J. Mech. Phys. Solids 51 (5), 765–793. doi:10.1007/978-3-642-18756-8_11.

Tanaka, K., Kobayashi, S., Sato, Y., 1986. Thermomechanics of transformation pseudoelasticity and shape memory effect in alloys. Int. J. Plast. 2 (1), 59–72. doi:10.1016/0749-6419(86)90016-1.

Triantafyllidis, N., Bardenhagen, S., 1993. On higher order gradient continuum theories in 1-d nonlinear elasticity. Derivation from and comparison to the corresponding discrete models. J. Elast. 33 (3), 259–293. doi:10.1007/BF00043251.

Truskinovsky, L., Vainchtein, A., 2004. The origin of nucleation peak in transformation plasticity. J. Mech. Phys. Solids 52 (6), 1421–1446. doi:10.1016/j.jmps.2003.09.034.

Weiner, J.H., 1983. Statistical Mechanics of Elasticity. Dover Publications. doi:10/0486422607

Wu, H., 2006. Molecular dynamics study on mechanics of metal nanowire. Mech. Res. Commun. 33 (1), 9–16. doi:10.1016/j.euromechsol.2005.11.008.

Xu, T., Lannon, H., Wolf, S., Nakamura, F., Brujic, J., 2013. Domain-domain interactions in filamin A (16-23) impose a hierarchy of unfolding forces. Biophys. J. 104 (9), 2022–2030. doi:10.1016/j.bpj.2013.03.034.

Zhang, Y., Shim, H.W., Huang, H., 2008. Size dependence of twin formation energy in cubic SiC at the nanoscale. Appl. Phys. Lett. 92 (26), 261908. doi:10.1063/1.2953976.